osteoclast formation in murine bone marrow cultures from adult mice: Antagonism by noggin. J Bone Miner Res **15**:663–673.
32. Aspenberg P, Jeppsson C, Economides AN 2001 The bone morphogenetic proteins antagonist Noggin inhibits membranous ossification. J Bone Miner Res **16**:497–500.
33. Canalis E, Economides AN, Gazzerro E 2003 Bone morphogenetic proteins, their antagonists, and the skeleton. Endocr Rev **24**:218–235.
34. Wu XB, Li Y, Schneider A, Yu W, Rajendren G, Iqbal J, Yamamoto M, Alam M, Brunet LJ, Blair HC, Zaidi M, Abe E 2003 Impaired osteoblastic differentiation, reduced bone formation, and severe osteoporosis in noggin-overexpressing mice. J Clin Invest **112**:924–934.

Address reprint requests to:
Noriyuki Tsumaki, MD, PhD
Department of Orthopaedic Surgery
Osaka University Graduate School of Medicine
2-2 Yamadaoka, Suita
Osaka 565-0871, Japan
E-mail: tsumaki-n@umin.ac.jp

Received in original form October 26, 2005; revised form March 17, 2006; accepted April 20, 2006.

J Bone Miner Metab (2006) 24:368–372
DOI 10.1007/s00774-006-0701-4

ORIGINAL ARTICLE

Takuma Matsubara · Akira Myoui · Fumiyo Ikeda
Kenji Hata · Hideki Yoshikawa · Riko Nishimura
Toshiyuki Yoneda

Critical role of cortactin in actin ring formation and osteoclastic bone resorption

Received: January 4, 2006 / Accepted: March 29, 2006

Abstract Tyrosine kinase c-Src plays an essential role in ruffled border formation and bone resorption in osteoclasts; however, it is unclear how c-Src controls ruffled border formation during bone resorption. To address this question, we investigated the role of cortactin, a c-Src substrate, in osteoclasts. We found that cortactin showed colocalization with c-Src and actin rings in osteoclasts. Overexpression of cortactin stimulated actin ring formation in RAW 264.7 cells. In contrast, overexpression of Csk inhibited tyrosine phosphorylation of cortactin and binding of cortactin to c-Src. More importantly, overexertion of a mutant cortactin strongly suppressed actin ring formation and bone resorbing activity in osteoclasts. Collectively, our data indicate that cortactin controls osteoclastic bone resorption by regulating actin organization.

Key words cortactin · c-Src · osteoclast

Introduction

A tyrosine kinase, c-Src, plays a critical role in actin organization and cytoskeletal structure [1]. Mice deficient in the *c-Src* gene manifest an osteopetrotic phenotype due to disorder of the ruffled border formation that is essential for osteoclastic bone resorption [2,3]. Consistent with these in vivo findings, osteoclasts isolated from c-Src-deficient mice fail to form actin rings, which are structures corresponding to the clear zone [4,5]. These findings suggest that c-Src regulates actin organization and exhibits an essential role in the bone resorbing activity of osteoclasts. However, the molecular mechanisms by which c-Src controls bone resorption in osteoclasts is unknown.

Cortactin has been identified as a c-Src substrate [6]. Cortactin regulates actin polymerization by activating the actin-related protein2/3 (Arp2/3) complex and stabilizes the cortical actin network [7]. Recently, Arp2/3 was shown to be required for actin ring formation in osteoclasts [8]. We, therefore, speculated that cortactin is implicated in regulation of osteoclastic bone resorption as a downstream signaling molecule for c-Src. We found that cortactin shows almost identical localization with actin rings in osteoclasts. Furthermore, overexpression of mutant cortactin impaired actin ring formation and the bone resorbing activity of osteoclasts. Our findings support the proposition that cortactin conducts actin organization in osteoclasts and is required for osteoclastic bone resorption.

T. Matsubara · F. Ikeda · K. Hata · R. Nishimura (✉) · T. Yoneda
Department of Molecular and Cellular Biochemistry, Graduate School of Dentistry, Osaka University, 1-8 Yamadaoka, Suita 565-0871, Japan
Tel. +81-6-6879-2887; Fax +81-6-6879-2890
e-mail: rikonisi@dent.osaka-u.ac.jp

A. Myoui · H. Yoshikawa
Department of Orthopaedics, Graduate School of Medicine, Osaka University, Osaka, Japan

Materials and methods

Cell and reagents

A monocytic cell line, RAW 264.7, was purchased from the RIKEN cell bank (Tsukuba, Ibaraki, Japan) and cultured in minimum essential medium eagle, alpha modification (α-MEM) containing 10% fetal calf serum (FCS) (Valley Biomedical, Winchester, VA, USA). Soluble receptor activator of NF-kappaB ligand (sRANKL) and macrophage colony-stimulating factor (M-CSF) were purchased from PeproTech EC (Rocky Hill, NJ, USA) and Green Cross (Osaka, Japan), respectably. Anti-c-Src and anticortactin antibodies were purchased from Oncogene Science (Cambridge, MA, USA) and Upstate Biotechnology (Lake Placid, NY, USA), respectively. 4,6 diamidino-2-phenylindole (DAPI) was purchased from Molecular Probes (Eugene, OR, USA) and rhodamine-labeled phalloidin from Fluka (St. Louis, MI, USA). c-Src and cortactin cDNA were kindly donated by Drs. Harold E. Varmus and Thomas Parsons. To generate a mutant cortactin lacking the actin binding domain, PCR products were synthesized and then subcloned into

pcDNA3 (Invitrogen, Carlsbad, CA, USA) and tagged with a Flag epitope at the N-terminus. The sequence of the construct was confirmed by DNA sequence analysis.

Osteoclast differentiation in vitro

Bone marrow cells or spleen cells were isolated from C57BL/6 mice (Nihon SLC, Hamamatsu, Shizuoka, Japan) and incubated with M-CSF (30 ng/ml) and sRANKL (100 ng/ml) for 6 days. After 6 days, the cells were analyzed by tartrate-resistant acid phosphate (TRAP) staining, and TRAP-positive multinucleated cells were counted as osteoclasts. RAW 264.7 cells were incubated in the presence of sRANKL (20 ng/ml) for 4 days.

Pit formation assay

To examine the function of TRAP-positive cells derived from spleen cells or bone marrow cells, we induced osteoclast formation on dentin slices. After 6 days of culture, cells were removed from the dentin slices. The resorption pits formed on dentine slices were stained with tolluidine blue. The pit formation areas were quantified using an image analysis system, Image-Pro Plus (Silver Spring, MD, USA).

Immunoprecipitation and immunoblotting analysis

The cells were washed three times with ice-cold phosphate-buffered saline (PBS) and solubilized in lysis buffer [20 mM 2-[4-(2-Hydroxyethyl)-1-piperazinyl]ethanesulfonic acid (Hepes) (pH 7.4), 150 mM NaCl, 1 mM ethyleneglycol bis (2-aminoethylether)tetraacetic acid (EGTA), 1.5 mM $MgCl_2$, 10% glycerol, 1% Triton X-100, 10 μg/ml aprotinin, 10 μg/ml leupeptin, 1 mM phenylmethylsulfonyl fluoride (PMSF), and 0.2 mM sodium orthovanadate]. The lysates were centrifuged for 15 min at 4°C at 16000 g and incubated with antibodies for 4 h at 4°C, followed by immunoprecipitation with protein A-sepharose (Zymed, CA, USA) or protein G-agarose (Boehringer Mannheim, Ingelheim, Germany). Immunoprecipitates were washed five times with lysis buffer and boiled in sodium dodecyl sulfate (SDS) sample buffer containing 0.5 M beta-mercaptoethanol; supernatants were recovered as immunoprecipitate samples. The immunoprecipitates or proteins isolated from RAW 264.7 cells were loaded for sodium dodecyl sulfate-polyacrylamide gel electrophoresis (SDS-PAGE) and immunoblotting was performed using specific antibodies. In all immunoblotting analyses, we also confirmed that equal amounts of proteins were loaded by staining the transferred membrane with Ponceau S.

Generation of adenovirus

The recombinant adenoviruses carrying c-Src, wild-type, or mutant cortactin were constructed by recombination between the expression cosmid cassette and the parental virus genome in 293 cells as previously described [9]. The viruses were confirmed to retain no proliferative activity in the cells other than the 293 cells. Titers of the viruses were determined using the modified point assay [9].

Immunocytochemistry

Cells were washed three times with ice-cold PBS, fixed with 3.8% paraformaldehyde-PBS, and permeabilized by incubation for 15 min with 0.1% Triton-PBS. The cells were blocked with 1% bovine serum albumin-phosphate buffered saline (BSA-PBS), incubated with anti-c-Src or anticortactin antibody for 2 h, washed six times with 0.1% Triton-PBS, and finally incubated with rhodamine-conjugated antimouse immunogloburin G (IgG) antibody. The cells were extensively washed with PBS and visualized using a fluorescence microscope (Carl Zeiss, Hallbergmoos, Germany).

Results

To understand the role of cortactin in osteoclasts, we first examined the cellular localization of cortactin. Immunocytochemical analyses demonstrated that cortactin was well localized in the actin rings of osteoclasts (Fig. 1A, B, C). In addition, cortactin showed a similar expression pattern to c-Src in osteoclasts (Fig. 1D, E, F). These data suggest that cortactin plays a role in actin ring formation in cooperation with c-Src. To examine the relationship between c-Src and cortactin, we next performed coimmunoprecipitation experiments using an osteoclastic precursor cell line RAW 264.7. Overexpression of cortactin induced tyrosine phosphorylation of cortactin and its association with c-Src in RAW 264.7 cells (Fig. 2). Importantly, overexpression of Csk, which suppresses c-Src function [10], markedly inhibited the association of cortactin with c-Src and the tyrosine phosphorylation of cortactin (Fig. 2). These data support the notion that cortactin functions as a downstream signaling molecule of c-Src.

To evaluate the functional role of cortactin in osteoclasts, we next examined the effect of cortactin on RAW 264.7 cells, which rarely form actin rings, even in the presence of sRANKL [9] (Fig. 3). Overexpression of c-Src clearly stimulated actin ring formation in RAW 264.7 cells (Fig. 3). Furthermore, overexpression of cortactin elicited formation of actin rings (Fig. 3), although cortactin-overexpressing RAW 264.7 cells exhibited little bone resorbing activity. These data indicate that cortactin is implicated in regulation of actin ring formation.

To further analyze the distinctive role of cortactin in osteoclasts, we generated a mutant of cortactin that lacks the actin binding domain (Fig. 4A), and overexpressed the mutant in osteoclasts using an adenovirus system [11]. As shown in Fig. 4B, overexpression of the mutant cortactin disrupted actin ring formation in osteoclasts. More importantly, osteoclastic bone resorption was strongly inhibited by the mutant cortactin (Fig. 4C). Together, the results indicate that cortactin plays a critical role in osteoclastic bone resorption by regulating actin ring formation.

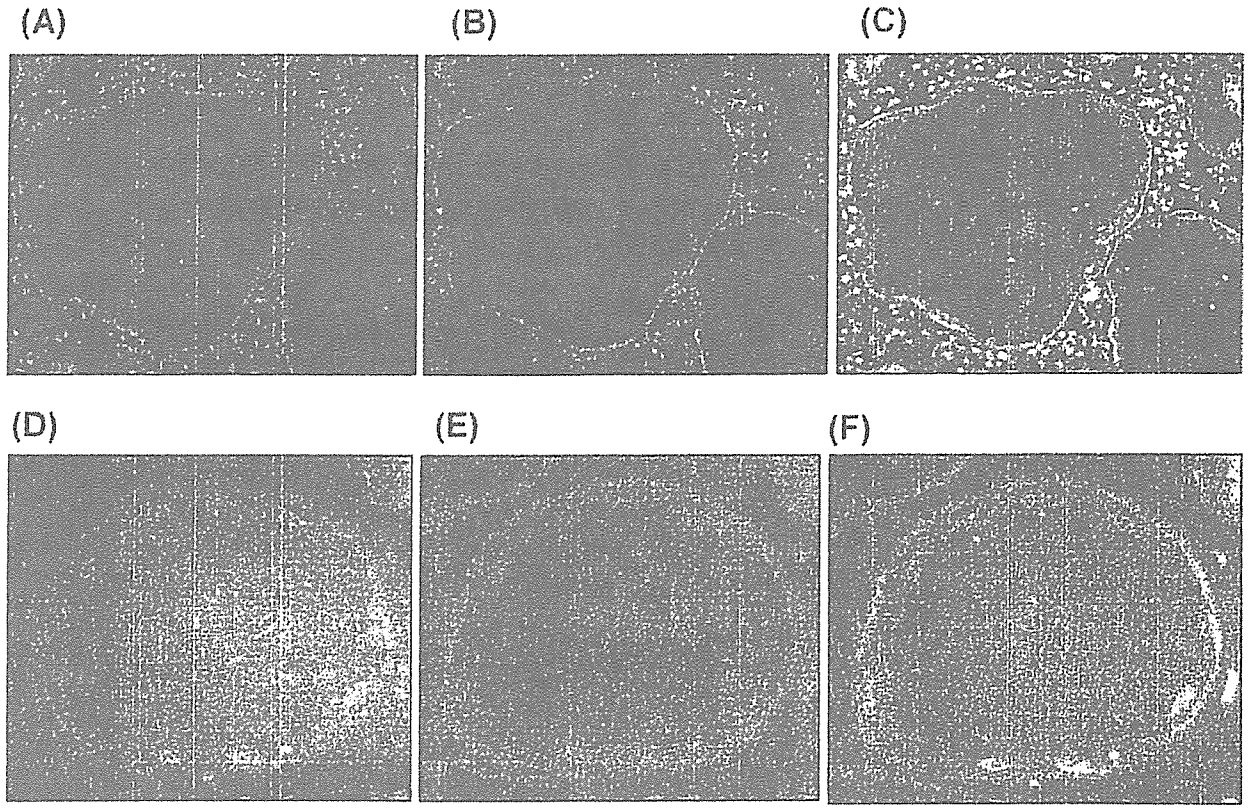

Fig. 1. Localization of cortactin in osteoclasts. Osteoclasts formed from mouse spleen cells were stained with anticortactin antibody (**A** and **D**), fluorescein isothiocyanate (FITC)-labeled phalloidin (**B**), and anti-c-Src antibody **E**. **C** and **F** are merged photographs of **A** and **B**, and **D** and **E**, respectively. ×1000

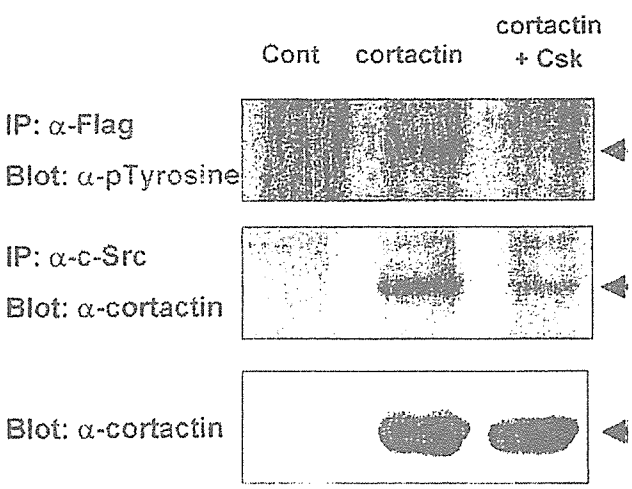

Fig. 2. Tyrosine-phosphorylation of cortactin and its association with c-Src. The lysates of RAW 264.7 cells infected with control adenovirus, or Flag-tagged cortactin with or without Csk adenoviruses, were immunoprecipitated with anti-Flag or c-Src antibody and immunoblotted with antiphosphotyrosine or anticortactin antibody, respectively. The expression of cortactin in the lysates was examined with anticortactin antibody (lower panels). *IP*, immunoprecipitation

Discussion

Several lines of evidence indicate that c-Src is an essential tyrosine kinase for osteoclastic bone resorption [2–4,12]. In this study, we showed that cortactin is expressed specifically in actin rings and is well colocalized with c-Src in osteoclasts. We also confirmed that cortactin functions as a c-Src substrate based on results of the binding of cortactin with c-Src and c-Src-dependent tyrosine phosphorylation. Furthermore, we indicated that overexpression of cortactin elicited formation of actin rings in RAW 264.7 cells that were differentiated into TRAP-positive osteoclasts by sRANKL. Finally, we found that a mutant of cortactin diminished both actin ring formation and bone resorption. Collectively, our data suggest the indispensable role of cortactin in osteoclast function.

Hurst et al. reported that the actin-related protein2/3 (Arp2/3) complex is essential for actin ring formation in osteoclasts [8]. Cortactin has been shown to control actin polymerization through Arp2/3 [13]. Considering that c-Src interacts with and controls cortactin [6], it is most likely that cortactin links c-Src signaling to Arp2/3 in osteoclasts, and thereby regulates actin polymerization. To support this proposed mechanism, we found that Csk, which is an inhibitory kinase for c-Src, inhibited tyrosine phosphorylation of cortactin, its association with c-Src and osteoclastic bone

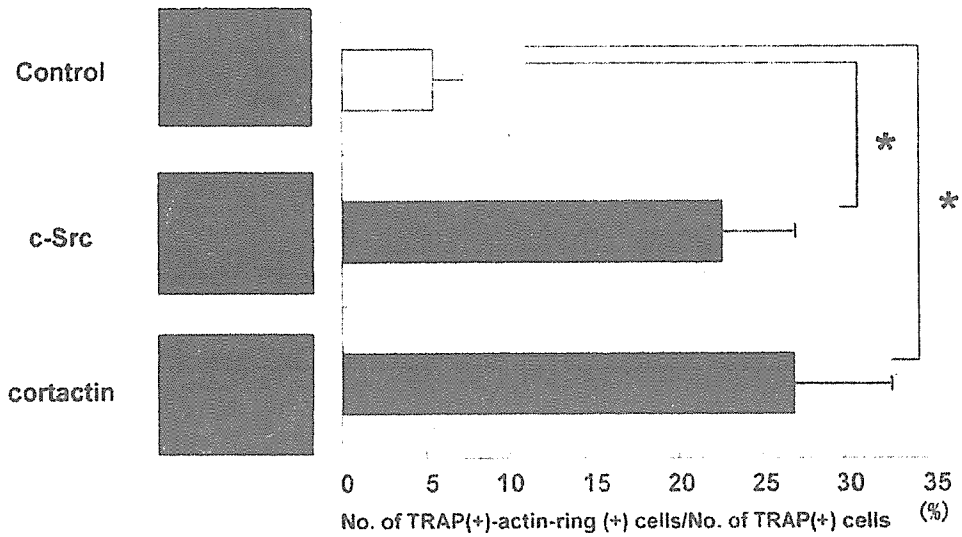

Fig. 3. Stimulation of actin ring formation of RAW 264.7 cells by cortactin. RAW 264.7 cells were cultured in the presence of soluble receptor activator of NF-kappaB ligand (sRANKL) (10 ng/ml) for 2 days, and infected with control, c-Src, or Flag-tagged cortactin adenovirus. Three days after infection, the cells were determined by tartrate-resistant acid phosphate (TRAP) staining and rhodamine-phalloidin. The number of TRAP-positive multinucleated cells and the number of TRAP-positive multinucleated cells that form actin rings are shown. The photographs show representative cells.

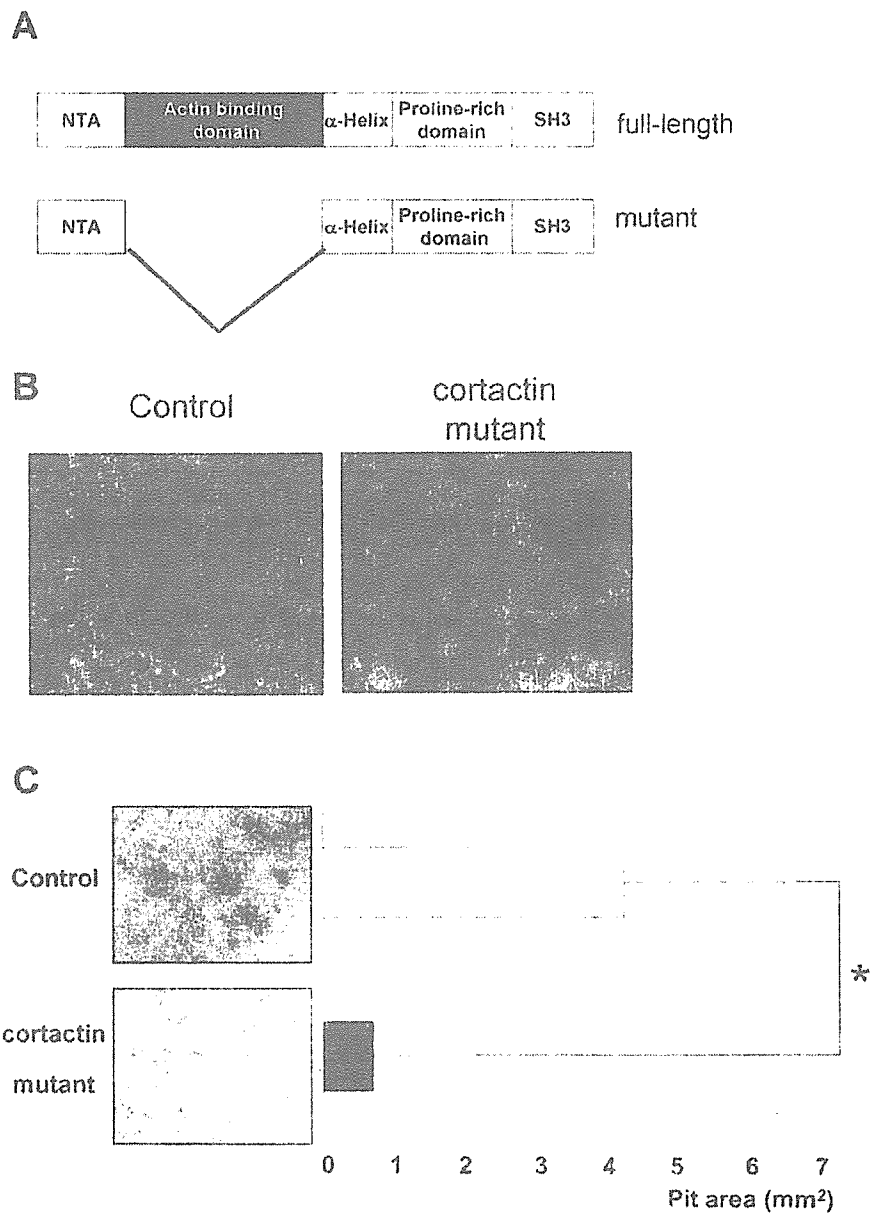

Fig. 4. Disruption of actin ring formation and bone resorption by a mutant cortactin. **A** Schematic diagram of a mutant cortactin. **B** Osteoclasts formed from mouse spleen cells were infected with control or mutant cortactin adenovirus, and 36 h after infection, the cells were stained with rhodamine-labeled phalloidin. **C** Mouse spleen cells were incubated with sRANKL (100 ng/ml) and macrophage colony-stimulating factor (M-CSF) (30 ng/ml) for 4 days and infected with control or mutant cortactin adenovirus; 2 days after infection, the pits were examined.

resorption (data not shown). Consistent with our results with the osteoclasts, Destaing et al. showed that cortactin is localized at podosomes of RAW 264.7-cell-derived osteoclasts [14]. However, they also clearly demonstrated that the turnover of cortactin is a few times slower than actin turnover [14]. Thus, it is likely that other components of the actin core are implicated in actin turnover in osteoclasts.

In conclusion, we have provided evidence that cortactin is an important signaling molecule that regulates actin ring formation and bone resorption in osteoclasts. We believe that our findings contribute to understanding the molecular mechanism of bone destruction by osteoclasts.

Acknowledgments We thank Drs. Harold E. Varmus and Thomas Parsons for providing c-Src and cortactin cDNA, respectively. This work was supported in part by the Ministry of Education, Science, Sports and Culture's Grant-in-Aid for Scientific Research A 11307041 (TY), B 15390560 (RN), and C 10671739 (RN), Grant-in-Aid for Scientific Research on Priority Areas B 12137205 (TY), and The 21st Century COE Program (TY, RN).

References

1. Frame MC, Fincham VJ, Carragher NO, Wyke JA (2002) v-Src's hold over actin and cell adhesions. Nat Rev Mol Cell Biol 3:233–245
2. Soriano P, Montgomery C, Geske R, Bradley A (1991) Targeted disruption of the c-src proto-oncogene leads to osteopetrosis in mice. Cell 64:693–702
3. Boyce BF, Yoneda T, Lowe C, Soriano P, Mundy GR (1992) Requirement of pp60c-src expression for osteoclasts to form ruffled borders and resorb bone in mice. J Clin Invest 90:1622–1627
4. Lowe C, Yoneda T, Boyce BF, Chen H, Mundy GR, Soriano P (1993) Osteopetrosis in Src-deficient mice is due to an autonomous defect of osteoclasts. Proc Natl Acad Sci USA 90:4485–4489
5. Miyazaki T, Neff L, Tanaka S, Horne WC, Baron R (2003) Regulation of cytochrome c oxidase activity by c-Src in osteoclasts. J Cell Biol 160:709–718
6. Wu H, Parsons JT (1993) Cortactin, an 80/85-kilodalton pp60src substrate, is a filamentous actin-binding protein enriched in the cell cortex. J Cell Biol 120:1417–1426
7. Li Y, Uruno T, Haudenschild C, Dudek SM, Garcia JG, Zhan X (2004) Interaction of cortactin and Arp2/3 complex is required for sphingosine-1-phosphate-induced endothelial cell remodeling. Exp Cell Res 298:107–121
8. Hurst IR, Zuo J, Jiang J, Holliday LS (2004) Actin-related protein 2/3 complex is required for actin ring formation. J Bone Miner Res 19:499–506
9. Ikeda F, Nishimura R, Matsubara T, Tanaka S, Inoue J, Reddy SV, Hata K, Yamashita K, Hiraga T, Watanabe T, Kukita T, Yoshioka K, Rao A, Yoneda T (2004) Critical roles of c-Jun signaling in regulation of NFAT family and RANKL-regulated osteoclast differentiation. J Clin Invest 114:475–484
10. Takayanagi H, Iizuka H, Juji T, Miyazaki T, Iizuka H, Takahashi T, Isshiki M, Okada M, Tanaka Y, Koshihara Y, Oda H, Kurokawa T, Nakamura K, Tanaka S (1999) Suppression of arthritic bone destruction by adenovirus-mediated csk gene transfer to synoviocytes and osteoclasts. J Clin Invest 104:137–146
11. Hata K, Nishimura R, Ueda M, Ikeda F, Matsubara T, Ichida F, Hisada K, Nokubi T, Yamaguchi A, Yoneda T (2005) A C/EBPbeta-enhancer binding protein beta isoform, liver-enriched inhibitory protein regulates commitment of osteoblasts and adipocytes. Mol Cell Biol 25:1971–1979
12. Horne WC, Sanjay A, Bruzzaniti A, Baron R (2005) The role(s) of Src kinase and Cbl proteins in the regulation of osteoclast differentiation and function. Immunol Rev 208:106–125
13. Zhu J, Zhou K, Hao JJ, Liu J, Smith N, Zhan X (2005) Regulation of cortactin/dynamin interaction by actin polymerization during the fission of clathrin-coated pits. J Cell Sci 118:807–817
14. Destaing O, Saltel F, Geminard JC, Jurdic P, Bard F (2003) Podosomes display actin turnover and dynamic self-organization in osteoclasts expressing actin-green fluorescent protein. Mol Biol Cell 14:407–416

Research article

Open Access

Inhibitory effect of ribbon-type NF-κB decoy oligodeoxynucleotides on osteoclast induction and activity *in vitro* and *in vivo*

Yasuo Kunugiza[1,2], Tetsuya Tomita[2], Naruya Tomita[3], Ryuichi Morishita[1] and Hideki Yoshikawa[2]

[1]Division of Clinical Gene Therapy, Osaka University Graduate School of Medicine, 2-2 Yamada-oka, Suita, Osaka 565-0871, Japan
[2]Department of Orthopaedics, Osaka University Graduate School of Medicine, 2-2 Yamada-oka, Suita, Osaka 565-0871, Japan
[3]Division of Nephrology, Department of Internal Medicine, Kawasaki Medical School, 577 Matsushima, Kurashiki, Okayama 701-0192, Japan

Corresponding author: Tetsuya Tomita, tomita@ort.med.osaka-u.ac.jp

Received: 11 Oct 2005 Revisions requested: 1 Dec 2005 Revisions received: 27 Feb 2006 Accepted: 29 May 2006 Published: 3 Jul 2006

Arthritis Research & Therapy 2006, 8:R103 (doi:10.1186/ar1980)
This article is online at: http://arthritis-research.com/content/8/4/R103

Abstract

In this study we examined the effect of ribbon-type (circular-type) NF-κB decoy oligodeoxynucleotides (RNODN) on osteoclast induction and activity. We extracted bone marrow cells from the femurs of rats and incubated non-adherent cells with receptor activator of nuclear factor κB ligand (RANKL) and macrophage colony-stimulating factor (M-CSF). First, transfer efficiency into osteoclasts and their precursors, resistance to exonuclease, and binding activity of decoy to NF-κB were examined. Next, to examine the effect of RNODN on osteoclast induction and activity, osteoclast differentiation and pit formation assays were performed. RNODN were injected into the ankle joints of rats with collagen-induced arthritis. Joint destruction and osteoclast activity were examined by histological study. The resistance of RNODN to exonuclease and their binding activity on NF-κB were both greater than those of phosphorothionated NF-κB decoy oligodeoxynucleotides. The absolute number of multinucleate cells scoring positive for tartrate-resistant acid phosphatase was significantly decreased in the RNODN-treated group. The average calcified matrix resorbed area was significantly decreased in the RNODN-treated group. Histological study showed marked suppression of joint destruction and osteoclast activity by intra-articular injection of RNODN. These results suggest the inhibitory effect of RNODN on the induction and activity of osteoclasts. Direct intra-articular injection of RNODN into the joints may be an effective strategy for the treatment of arthritis.

Introduction

Osteoclasts are multinucleate giant cells formed by the fusion of hematopoietic cells of the monocyte/macrophage lineage. They are the major resorptive cells of bone [1,2]. In the differentiation pathway of osteoclast progenitors into functionally active osteoclasts, macrophage colony-stimulating factor (M-CSF) is important in proliferation; both M-CSF and receptor activator of NF-κB ligand (RANKL) are essentially involved in differentiation, survival, and fusion; and RANKL enhances osteoclast function [3,4]. The expression of RANKL can be observed in synovial fibroblasts from patients with rheumatoid arthritis (RA) [5]. A crucial target of signaling by RANKL is the activation of NF-κB [6-9]. NF-κB is associated with the activation of osteoclasts and is important in the differentiation of osteoclast precursors [10]. Several studies indicate that selective inhibition of NF-κB in osteoclast precursors prevents osteoclast differentiation and function *in vitro* and *in vivo* [11,12]. Mice deficient in both the p50 and p65 subunits of NF-κB develop osteopetrosis because of a defect in osteoclast differentiation [13,14]. Recently the importance of the IκB kinase (IKK) β subunit as a transducer of signals from RANK to NF-κB for inflammation-induced bone loss and osteoclastogenesis *in vivo* was reported [15].

RA is a chronic inflammatory disease of unknown etiology, characterized by articular inflammation associated with

FCS = fetal calf serum; FITC = fluorescein isothiocyanate; IL = interleukin; M-CSF = macrophage colony-stimulating factor; NF-κB = nuclear factor-κB; ODN = oligodeoxynucleotide; PBS = phosphate-buffered saline; PNODN = phosphorothionate double-stranded NF-κB decoy ODN; PSODN = phosphorothionate double-stranded scrambled decoy ODN; RA = rheumatoid arthritis; RANKL = receptor activator of NF-κB ligand; RNODN = ribbon-type NF-κB decoy ODN; RSODN = ribbon-type scrambled decoy ODN; TNF = tumor necrosis factor; TRAP = tartrate-resistant acid phosphatase.

abnormal immune responses and pronounced synovial hyperplasia. Synovial macrophages are capable of differentiating into osteoclasts; the osteoclasts generated within the synovial membrane are probably involved in bone destruction *in vivo* [16]. Multinucleate cells scoring positive for tartrate-resistant acid phosphatase (TRAP) were also induced from CD14-positive cells in the synovial fluid from patients with RA [17]. TRAP-positive multinucleate cells are present in the bone erosion area of patients with RA [18] and also in the bone erosion area of a mouse arthritis model [19,20]. Although the precise mechanism of joint destruction has not been elucidated, osteoclasts seem to have a pivotal role in the joints of patients with RA.

Specific DNA sequences have been used successfully as decoys for binding specific transcription factors, rendering the transcription factors incapable of subsequent binding to the promoter region of target genes [21,22]. This approach has been shown to be effective in modulating gene expression *in vitro* and *in vivo*. The applications of the decoy oligodeoxynucleotides (ODN) strategy against NF-κB have been reported in several studies [23-26]. However, one of the major limitations of the decoy ODN approach is the rapid degradation of phosphodiester ODN by intracellular nucleases. Previously, circular dumbbell double-stranded decoy ODN (we call these ribbon-type decoy ODN) were developed to resolve these issues [27,28]. According to the previous reports, ribbon-type decoy ODN tend to bind more specifically to the transcription factors and have stronger resistance to exonuclease [29,30]. In this study, we tried to use ribbon-type NF-κB decoy ODN for inhibiting the expression of NF-κB, leading to the inhibition of osteoclast induction and activity.

Materials and methods

Materials

Ribbon-type decoy ODN and phosphorothionated double-stranded decoy ODN were purchased from Gene Design (Osaka, Japan). Mouse RANKL and mouse M-CSF were purchased from Wako (Tokyo, Japan). Lewis rats were purchased from Clea Japan (Osaka, Japan). Bovine type II collagen was purchased from Cosmo Bio (Tokyo, Japan) and Freund's incomplete adjuvant from Sigma (Munich, Germany).

Construction of ribbon-type decoy ODN and phosphorothionated double-stranded decoy ODN

The sequences of ribbon-type decoy ODN and phosphorothionated double-stranded decoy ODN are as follows (consensus sequences are shown in bold): ribbon-type NF-κB decoy ODN (RNODN), 5'-TCAAGGAAAACCTTGAAG-GGATTTCCCTCCAAAAGGAGGGAAATCCCT-3' ; ribbon-type scrambled decoy ODN (RSODN), 5'-TAGCCAAAAGGCTAAGTCAGGTACGGCAAAAAATT-GCCGTACCTGACT-3' ; phosphorothionated double-stranded NF-κB decoy ODN (PNODN), 5'-CCTTGAAG-GGATTTCCCTCC-3' and 3'-GGAACTTCCCTAAAG-GGAGG-5' ; and phosphorothionate double-stranded scrambled decoy ODN (PSODN) 5'-TTGCCGTACCTGACT-TAGCC-3' and 3'-AACGGCATGGACTGAATCGG-5' (Figure 1). Decoy ODN containing the NF-κB consensus sequence has been shown to bind the NF-κB transcription factor [24]. PNODN and PSODN were annealed for 2 hours with a steady temperature decrease from 70°C to 25°C. One unit of T4 DNA ligase was added to the mixture, followed by incubation for 24 hours at 22°C to generate a covalently ligated RNODN.

Resistance to exonuclease

To check resistance for exonuclease, electrophoresis of RNODN and PNODN was performed. In brief, 3 μg of RNODN or PNODN was incubated with exonuclease III at 37°C for 2 hours and then at 65°C for 5 minutes. The solution containing ODN was resolved by electrophoresis on a 19% acrylamide gel.

Estimation of binding activity

The binding activity of RNODN was examined by using Mercury Transfactor Kits for NF-κB p65 (BD Bioscience, Clontech, Palo Alto, CA, USA) as oligonucleotide competition assays. Kits contain a 96-well format in which wells are coated with an oligonucleotide containing the NF-κB p65 consensus binding sequence. The quantity of nuclear extract binding to the oligonucleotide of the wells is correlated with an increase in signal. An increase in the amount of competitor oligonucleotide corresponds to a decrease in signal because transcription factor binding decreases as the competitor keeps it away from the oligonucleotide-coated surface of the *trans*-Factor well. We estimated the binding activity of oligonucleotides by incubating the same amounts of nuclear protein and various oligonucleotides. An aliquot (30 μg) of TNF-α-stimulated HeLa nuclear extract (Active Motif, Carlsbad, CA, USA) was incubated with decoy ODN (15, 30, and 45 nM) in *trans*-Factor wells for 60 minutes at room temperature. Wells were incubated with primary and secondary antibodies, and the absorbance of the plate was measured with a microplate reader (Model 680; Bio-Rad, Hercules, CA, USA).

Osteoclast differentiation assay

Bone marrow cells were obtained by flushing femurs of 6-week-old female Lewis rats and were seeded at 2×10^7 cells per 10 cm Petri dish, then cultured in α-minimal essential medium containing 10% FCS and 1% penicillin/streptomycin. One day after the treatment, non-adherent cells were seeded again and cultured in α-minimal essential medium containing 10% FCS, 1% penicillin/streptomycin, and 20 ng/ml M-CSF in Lab-Tek eight-well chamber slides (Nalge Nunc, New York, NY, USA) at a density of 2×10^5 cells per well. Two days after the incubation, cells were cultured with 100 ng/ml RANKL and 20 ng/ml M-CSF for 7 days. On days 1, 3, and 5 various decoy ODNs were transiently transferred. Then the cells were washed and stained with a commercial TRAP staining kit (Cell

Figure 1

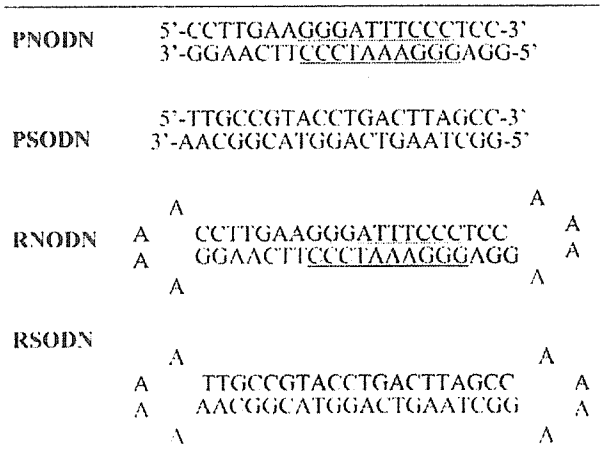

Structures and sequences of the decoy oligodeoxynucleotides used in this study. PNODN and RNODN (phosphorothionated decoy oligodeoxynucleotides) contain the NF-κB-binding site in its double-stranded lesion (consensus sequences are underlined).

Garage, Tokyo, Japan). The number of TRAP-positive multinuclear (three or more nuclei) cells was counted.

Pit formation assay

To examine the effect of RNODN on resorbing activity, cells were cultured on BD BioCoat osteologic calcium hydroxyapatite-coated slides (BD Biosciences, Bedford, MA, USA) in a 5% CO_2 incubator. The non-adherent bone marrow cells were seeded at a density of 10^5 cells per well. After incubation for 2 days with 20 ng/ml M-CSF, cells were cultured with 100 ng/ml RANKL and 20 ng/ml M-CSF. On days 3, 5, and 7 various decoy ODNs were transiently transferred, and on day 8 cells were washed vigorously and the calcified matrix resorption area on each disc was measured with a Mac SCOPE image analyzer, version 2.51 (Mitani, Fukui, Japan).

Immunofluorescence staining

Cells were fixed in 4% paraformaldehyde for 20 minutes at 37°C and treated with 0.5% Triton X-100 for 5 minutes. Cells were then blocked for 30 minutes with 2% goat serum/PBS and incubated in 4 μg/ml rabbit polyclonal antibody against NFATc1 (sc-13033; Santa Cruz biotechnology, Santa Cruz, CA, USA) at 4°C for 16 hours and 400 ng/ml Alexa 488 goat anti-rabbit IgG (A-12373; Invitrogen Molecular Probes, Carlsbad, CA, USA) at room temperature for 60 minutes. The density of fluorescence was estimated by calculating the area of fluorescent cells by NIH image software.

Induction of arthritis by collagen in rats

This experimental study was performed in accordance with the recommendations in the Guide for the Care and Use of Laboratory Animals of National Institutes of Health (NIH). The protocol was approved by the committee on the Ethics of Animal Experiments in Osaka University. Arthritis was induced by collagen with the use of the modified method described by Trentham and colleagues [31]. In brief, 6-week-old female Lewis rats were immunized intradermally with 0.5 mg of bovine type II collagen, which was dissolved in 0.5 ml of 0.1 M acetic acid at 4°C and emulsified in 0.5 ml of cold Freund's incomplete adjuvant. On day 7, the rats received an intradermal booster injection of half the volume of the first immunization. Onset of arthritis in the ankle joints could be usually recognized visually between days 10 and 14. All rats in which the onset of arthritis could not be recognized visually by day 14 were excluded from this study.

Figure 2

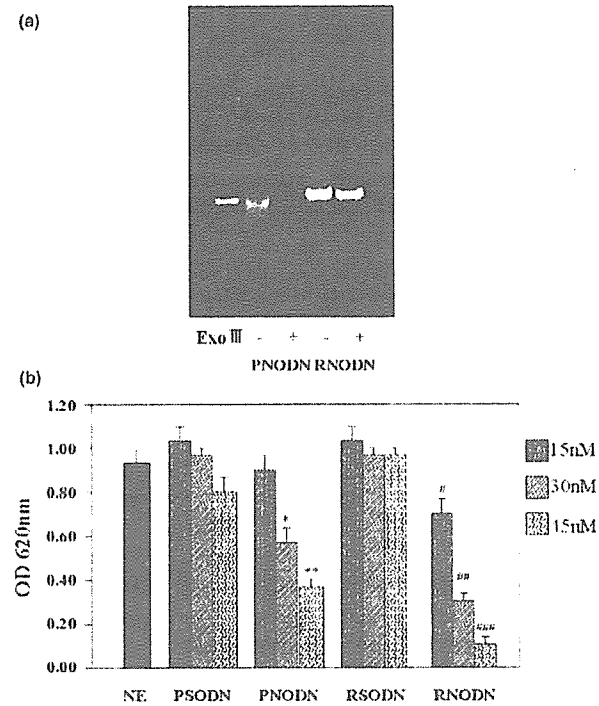

The stability and binding activity of RNODN and PNODN. (a) Stability of phosphorothionate double-stranded NF-κB decoy oligodeoxynucleotide (PNODN) and ribbon-type NF-κB decoy oligodeoxynucleotide (RNODN) in the presence of exonuclease III. (b) Effects of various decoys on binding activity towards NF-κB. The binding activity of decoy oligodeoxynucleotides (ODNs) reflected their ability to decrease absorbance. NE, nuclear extract without treatment of decoy ODN. (n = 5 per group; $^{*}p < 0.05$, $^{**}p < 0.01$, $^{\#}p < 0.05$, $^{\#\#}p < 0.01$, $^{\#\#\#}p < 0.001$ compared with nuclear extract without treatment of decoy ODN.)

In vivo transfer of fluorescein isothiocyanate (FITC)-labeled RNODN

To examine the localization of RNODN delivery, 50 μg of FITC-labeled RNODN were injected intra-articularly. One day after transfer, synovial tissues were extracted and fixed. Cryostat sections of synovial cells were observed by ultraviolet microscopy (T6300; Nikon, Tokyo, Japan). The sections were also stained with 4',6-diamidino-2-phenylindole.

Figure 1

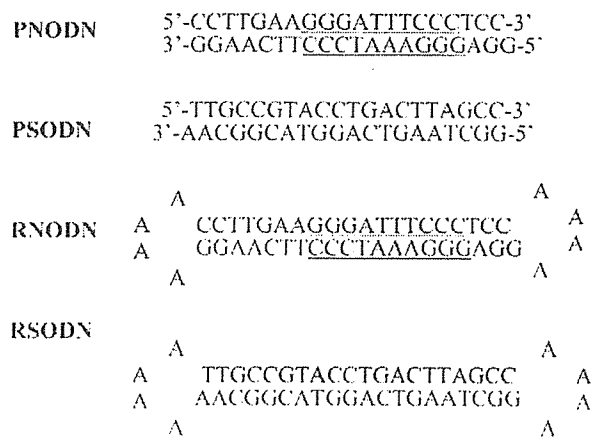

Structures and sequences of the decoy oligodeoxynucleotides used in this study. PNODN and RNODN (phosphorothionated decoy oligodeoxynucleotides) contain the NF-κB-binding site in its double-stranded lesion (consensus sequences are underlined).

Garage, Tokyo, Japan). The number of TRAP-positive multinuclear (three or more nuclei) cells was counted.

Pit formation assay

To examine the effect of RNODN on resorbing activity, cells were cultured on BD BioCoat osteologic calcium hydroxyapatite-coated slides (BD Biosciences, Bedford, MA, USA) in a 5% CO_2 incubator. The non-adherent bone marrow cells were seeded at a density of 10^5 cells per well. After incubation for 2 days with 20 ng/ml M-CSF, cells were cultured with 100 ng/ml RANKL and 20 ng/ml M-CSF. On days 3, 5, and 7 various decoy ODNs were transiently transferred, and on day 8 cells were washed vigorously and the calcified matrix resorption area on each disc was measured with a Mac SCOPE image analyzer, version 2.51 (Mitani, Fukui, Japan).

Immunofluorescence staining

Cells were fixed in 4% paraformaldehyde for 20 minutes at 37°C and treated with 0.5% Triton X-100 for 5 minutes. Cells were then blocked for 30 minutes with 2% goat serum/PBS and incubated in 4 μg/ml rabbit polyclonal antibody against NFATc1 (sc-13033; Santa Cruz biotechnology, Santa Cruz, CA, USA) at 4°C for 16 hours and 400 ng/ml Alexa 488 goat anti-rabbit IgG (A-12373; Invitrogen Molecular Probes, Carlsbad, CA, USA) at room temperature for 60 minutes. The density of fluorescence was estimated by calculating the area of fluorescent cells by NIH image software.

Induction of arthritis by collagen in rats

This experimental study was performed in accordance with the recommendations in the Guide for the Care and Use of Laboratory Animals of National Institutes of Health (NIH). The protocol was approved by the committee on the Ethics of Animal Experiments in Osaka University. Arthritis was induced by collagen with the use of the modified method described by Trentham and colleagues [31]. In brief, 6-week-old female Lewis rats were immunized intradermally with 0.5 mg of bovine type II collagen, which was dissolved in 0.5 ml of 0.1 M acetic acid at 4°C and emulsified in 0.5 ml of cold Freund's incomplete adjuvant. On day 7, the rats received an intradermal booster injection of half the volume of the first immunization. Onset of arthritis in the ankle joints could be usually recognized visually between days 10 and 14. All rats in which the onset of arthritis could not be recognized visually by day 14 were excluded from this study.

Figure 2

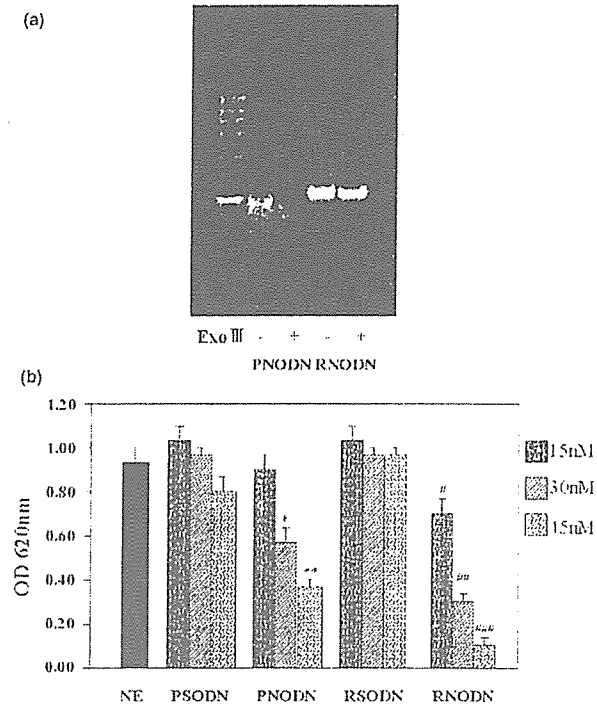

The stability and binding activity of RNODN and PNODN. (a) Stability of phosphorothionate double-stranded NF-κB decoy oligodeoxynucleotide (PNODN) and ribbon-type NF-κB decoy oligodeoxynucleotide (RNODN) in the presence of exonuclease III. (b) Effects of various decoys on binding activity towards NF-κB. The binding activity of decoy oligodeoxynucleotides (ODNs) reflected their ability to decrease absorbance. NE, nuclear extract without treatment of decoy ODN. (n = 5 per group; $^{*}p < 0.05$, $^{**}p < 0.01$, $^{\#}p < 0.05$, $^{\#\#}p < 0.01$, $^{\#\#\#}p < 0.001$ compared with nuclear extract without treatment of decoy ODN.)

In vivo transfer of fluorescein isothiocyanate (FITC)-labeled RNODN

To examine the localization of RNODN delivery, 50 μg of FITC-labeled RNODN were injected intra-articularly. One day after transfer, synovial tissues were extracted and fixed. Cryostat sections of synovial cells were observed by ultraviolet microscopy (T6300; Nikon, Tokyo, Japan). The sections were also stained with 4',6-diamidino-2-phenylindole.

Figure 4

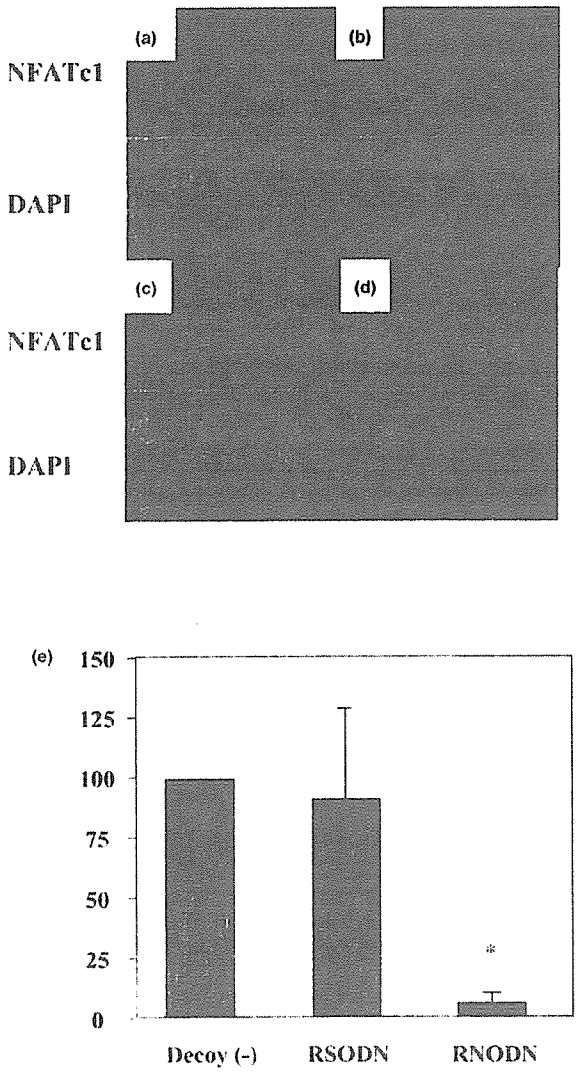

Expression of NFATc1 protein in osteoclast precursor cells. **(a-d)** Immunohistochemistry of NFATc1 protein with specific antibody in osteoclast precursor cells. Bone marrow macrophages were incubated with M-CSF/RANKL for 48 hours after incubation with ribbon-type scrambled decoy oligodeoxynucleotide (RSODN) (c) or ribbon-type NF-κB decoy oligodeoxynucleotide (RNODN) (d), or were untreated alone (b). (a) Without reaction with primary antibody. The expression of NFATc1 by immunofluorescence is shown in each upper panel. Nuclei stained with 4',6-diamidino-2-phenylindole are shown in each lower panel. Original magnification × 100. **(e)** Measurement of fluorescent area of osteoclast precursor cells. The areas of fluorescent cells in RSODN-treated and RNODN-treated groups are shown as percentages over that of the untreated group. ($n = 5$ per group; $^*p < 0.001$ compared with the RSODN-treated group.)

Results

Stability of RNODN

In this study we used RNODNs to improve stability to exonuclease. Initially, the structural stability of decoy ODN was examined by the ability to resist degradation in the presence of exonuclease III. The primary cause of degradation of standard DNA oligomers in biological applications is a 3'-exonuclease activity found in cells [33,34]. RNODN showed high resistance to exonuclease III and was observed as a major band in gel electrophoresis. In comparison with RNODN, PNODN was degraded after incubation in the presence of exonuclease III (Figure 2a).

Binding activity of RNODNs on NF-κB

To examine the binding activity of RNODN on the NF-κB protein, an *in vitro* competition assay was performed with Mercury Transfactor Kits for NF-κB p65 (Figure 2b). An increase in the concentration of unbound NF-κB protein was accompanied by a corresponding increase in absorbance. The binding activity of decoy ODNs reflected their ability to decrease the absorbance level. The result of calculating the absorbance of each group is shown as a percentage over that of the untreated group. When PNODN or RNODN was used as a competitor oligonucleotide at 30 or 45 nM, a significant decrease in absorbance was confirmed against the absorbance of nuclear extract without competitor oligonucleotides. A stronger competitive effect was observed when RNODN was used than with PNODN. At a concentration of 15 nM, the competitive effect was observed only in the RNODN-treated group. When RSODN or PSODN was used as a competitor oligonucleotide, the decrease in absorbance was minimal compared with that of nuclear extract without competitor oligonucleotides. The result shows that RNODN has specific and strong binding activity on the NF-κB protein.

RNODN inhibits RANKL-induced osteoclastogenesis

To examine the effects of RNODN on osteoclastogenesis *in vitro*, bone marrow macrophages were incubated with decoy in the presence of RANKL and M-CSF (Figure 3a–c). The number of TRAP-positive multinuclear cells in the untreated group and in the RSODN-treated and RNODN-treated groups were 124.2 ± 34.6, 126.2 ± 45.5, and 5.2 ± 1.9, respectively (mean ± SD; Figure 3d). Osteoclastogenesis induced by RANKL was inhibited by incubation with RNODN ($p < 0.001$ compared with the RSODN-treated group). The inhibitory effect was not observed when cells were incubated with RSODN (Figure 3).

RNODN inhibits RANKL-induced pit formation

To examine the inhibitory effects of RNODN on the activation of osteoclasts, a pit formation assay was performed (Figure 3e–g). The calcified matrix resorption area in the untreated group and in the RSODN-treated and RNODN-treated groups were 1.03 ± 0.12, 1.01 ± 0.12, and 0.36 ± 0.21 mm^2, respectively (mean ± SD; Figure 3h). Results showed that calcified matrix resorption by RANKL-induced osteoclast-like cells was significantly inhibited by incubation with RNODN ($p < 0.01$ compared with the RSODN-treated group). The inhibitory

Figure 5

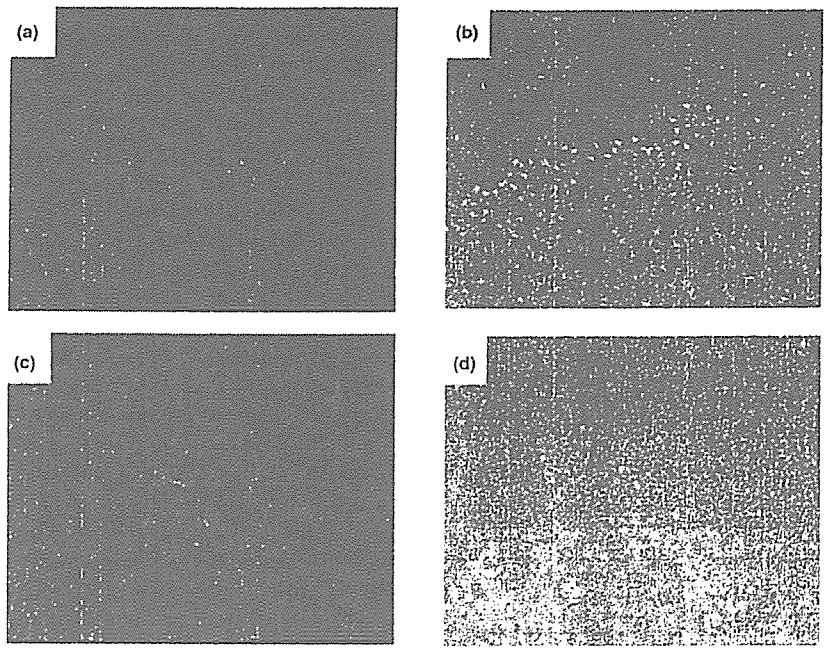

Representative findings of fluorescence microscopy of synovium transferred with FITC-labeled RNODN. **(a)** Synovium transferred with ribbon-type NF-κB decoy oligodeoxynucleotide (RNODN) not labeled with fluorescein isothiocyanate (FITC). **(b)** The sections were counterstained with 4',6-diamidino-2-phenylindole. **(c)** Synovium transferred with FITC-labeled RNODN. Original magnification × 200. **(d)** The sections were counterstained with 4',6-diamidino-2-phenylindole.

effect was not observed when cells were incubated with RSODN.

Downregulation of NFATc1 by RNODN

To clarify the mechanism underlying the inhibitory effect of RNODN on osteoclastogenesis, we examined the expression of the NFATc1 protein in bone marrow cells incubated with RANKL. NFATc1 is a master switch for regulating the terminal differentiation of osteoclasts, functioning downstream of RANKL [35]. As shown in Figure 4, the expression of NFATc1 in RANKL-stimulated bone marrow cells increased in accordance with the fusion of cells (Figure 4b). The results of calculating the area of fluorescent cells in RSODN-treated and RNODN-treated groups are shown as percentages over that of the untreated group. The data for each group (mean ± SD) are 90.0 ± 38.6% and 3.5 ± 3.2%, respectively (Figure 4e). The expression of NFATc1 was inhibited by incubation with RNODN ($p < 0.001$ compared with the RSODN-treated group; Figure 4d).

In vivo transfer of FITC-labeled RNODN into joint synovium

We performed *in vivo* transfer of FITC-labeled RNODN into rat ankle joints. Fluorescence was localized in synovial cells, especially the surface area (Figure 5c). Synovium transferred with decoy ODN not labeled with FITC showed no specific fluorescence (Figure 5a). The nucleus was stained with 4',6-diamidino-2-phenylindole (Figure 5b,d).

Inhibitory effects of intra-articular injection of RNODN on joint destruction and osteoclast activity in rats with CIA

To evaluate the effect of RNODN on joint destruction and osteoclast activation, we performed a histological analysis of the ankle joints treated with RNODN, RSODN, or PBS. Histologically, ankle joints of rats with CIA treated with PBS (Figure 6b) or RSODN (Figure 6c) showed pannus invasion and massive cellular infiltration of the synovium, with disruption of cartilage and subchondral bone. Conversely, ankle joints of rats with CIA treated with RNODN (Figure 6d) showed marked improvement in arthritis. The arthritis scores (mean ± SD) of PBS-treated joints, RSODN-treated joints, and RNODN-treated joints were 3.0 ± 0.7, 3.2 ± 0.8, and 1.8 ± 0.8, respectively (Table 1). The number of osteoclasts around the ankle joints was significantly smaller in RNODN-treated rats than in RSODN-treated or PBS-treated rats (Figure 6f,g). The numbers of osteoclasts in PBS-treated joints, RSODN-treated joints, and RNODN-treated joints were 142.8 ± 15.1, 153.8 ± 28.2, and 31.0 ± 27.3, respectively (Table 1). Figure 6a and Figure 6e show HE staining and TRAP staining of ankle joints in naive rats.

Figure 6

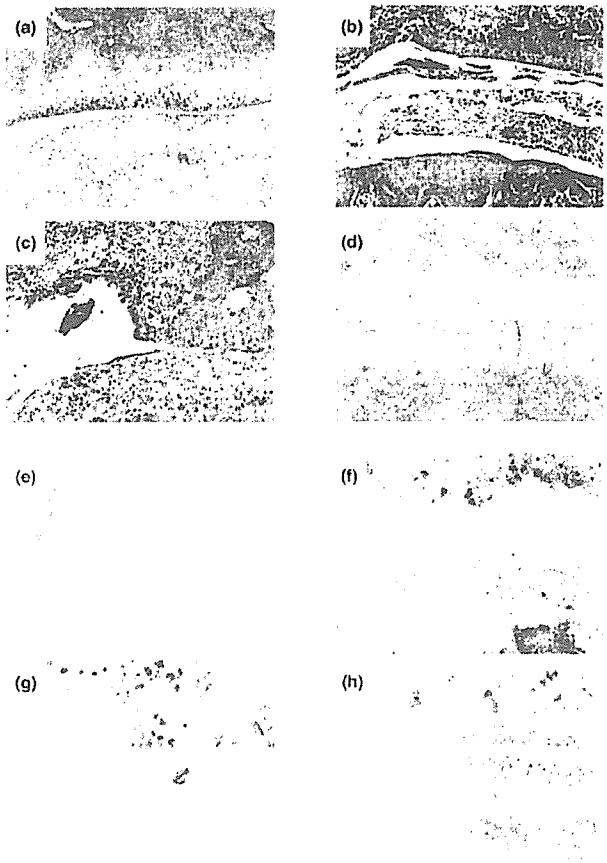

Histological analysis in the ankle joints of rats with collagen-induced arthritis (CIA) at day 35. Samples were stained with hematoxylin and eosin in (**a-d**) and with tartrate-resistant acid phosphatase [TRAP] in (**e-h**). (a) Naive rats had normal joints. (b) Ankle joints of rats with CIA treated with PBS showed pannus invasion and massive cellular infiltration of the synovium, with disruption of cartilage and subchondral bone. (c) Ankle joints of rats with CIA treated with ribbon-type scrambled decoy oligodeoxynucleotide (RSODN) also showed pannus invasion and massive cellular infiltration of the synovium, with disruption of cartilage and subchondral bone. (d) Ankle joints of rats with CIA treated with ribbon-type NF-κB decoy oligodeoxynucleotide (RNODN) also had nearly intact articular joints. (e) Ankle joints of naive rats had few TRAP-positive multinuclear cells. (f) Ankle joints of rats with CIA treated with PBS showed active resorption of cartilage and subchondral bone by pannus and synovium including TRAP-positive multinuclear cells. (g) Ankle joints of rats with CIA treated with RSODN also showed active resorption of cartilage and subchondral bone by pannus and synovium including TRAP-positive multinuclear cells. (h) TRAP-positive multinuclear cell formation was suppressed in ankle joints of rats with CIA treated with RNODN. Original magnifications × 100.

Discussion

The Rel/NF-κB family of transcription factors is induced in response to several signals. In unstimulated cells, NF-κB is associated in the cytoplasm with the inhibitory protein IκB. In response to an external signal, IκB is phosphorylated and degraded, releasing NF-κB to enter the nucleus and activate transcription [36,37]. The wide variety of genes regulated by NF-κB includes cytokines, chemokines, adhesion molecules, acute-phase proteins, and inducible effector enzymes. The important role of NF-κB in the differentiation and activation of osteoclasts has been mentioned previously [38]. Selective inhibition of NF-κB by several drugs blocks osteoclastogenesis [11,12]. In the present study we have shown that selective inhibition of NF-κB with a ribbon-type NF-κB decoy could suppress the differentiation and activation of RANKL-induced osteoclastogenesis. Transfection of decoy ODN corresponding to the *cis* sequences result in the attenuation of authentic cis-trans interaction, leading to the removal of *trans*-factors from the endogenous *cis*-element, with subsequent modulation of gene expression [39]. The principle of the transcription factor decoy approach is based on the reduction of promoter activity as a result of the inhibition of binding of a transcription factor to a specific sequence in the promoter region. This approach is relatively simple and can be targeted to specific tissues; decoy ODN can be more effective than antisense ODN in blocking constitutively expressed factors as well as multiple transcription factors that bind to the same *cis* element [39]. However, one of the major limitations of the decoy ODN approach is the rapid degradation of phosphodiester ODN by intracellular nucleases [40-42]. The lack of sequence specificity of phosphodiester ODN has been reported previously [29,43,44]. To overcome these issues, the circular dumbbell double-stranded decoy ODN was developed [42,45,46]. Circular dumbbell decoy ODN for AP-1 or E2F have been demonstrated to be more effective than conventional decoy ODN in previous studies [40,41]. In this study, RNODN showed higher resistance to exonuclease and stronger binding activity on NF-κB than PNODN, and we examined the effect of RNODN for the inhibition of osteoclast differentiation and activation. A previous report [47] showed the effect of decoy targeting NF-κB on apoptosis of human osteoclasts. In contrast to their results we were unable to show the specific effect of RNODN for apoptosis of rat osteoclasts. It is not yet clear whether NF-κB is responsible for the survival of osteoclasts [48].

In this study, we were able to transfer decoy ODN to adherent macrophage/monocyte-like cells and osteoclast-like cells without reagent. The possibility and effectiveness of ODN transfer into these cells have been reported previously [49]. The cellular uptake of ODN is reportedly achieved by a receptor-mediated endocytosis mechanism [50,51]. However, the exact mechanism of cellular uptake of naked DNA or ODN is still poorly defined [52]. The efficiency of internalizing naked DNA varies between cell types [52]. In our study, the effectiveness of ODN transfer was promoted in serum-free conditions. The size of the ribbon-type decoy is about 20 base pairs, which is small compared with the plasmid, so it may be easier for ODN to be transferred into osteoclasts or their precursors.

Table 1

Mean histological scores and osteoclast numbers of rats with collagen-induced arthritis

Group	Number of joints	Histological score	Osteoclast number
PBS injection	5	3.0 ± 0.7	142.8 ± 15.1
RSODN injection	5	3.2 ± 0.8	153.8 ± 28.2
RNODN injection	5	1.8 ± 0.8[a]	31.0 ± 37.3[b]

[a]$p < 0.01$ compared with PBS injection group; [b]$p < 0.01$ compared with PBS-injection group ($n = 5$ rats and $n = 5$ joints for each group). RNODN, ribbon-type NF-κB decoy oligodeoxynucleotide; RSODN, ribbon-type scrambled decoy oligodeoxynucleotide. Results are means ± SD.

In the pit formation assay of this study, we transferred the decoy on day 3. We were able to confirm TRAP-positive multinuclear cells on day 3 but the cells were not so large and it might be difficult to state that these cells were mature osteoclasts. It would have been better if we could have incubated mature osteoclasts on a hydroxyapatite-coated disc, but osteoclasts are easily damaged and it is technically difficult to subculture rat mature osteoclasts.

In the previous study, the gene encoding NFATc1, a member of the NFAT family of transcription factor genes, was found to be the most strongly induced transcription factor gene after stimulation by RANKL in osteoclast differentiation. NFATc1 autoamplifies its own gene, possibly by binding to its own promoter [35]. The AP-1 and NF-κB binding sites are present with the promoter region of the NFATc1 gene [53]. Recently, Takatsuna and colleagues showed that (-)-DHMEQ, a newly designed NF-κB inhibitor, inhibited RANKL-induced osteoclast differentiation in mouse bone marrow macrophages through the downregulation of NFATc1 [54]. In the present study the expression of NFATc1 was inhibited by treatment with RNODN.

The skeletal complications of RA consist of focal bone erosions and periarticular osteoporosis at sites of active inflammation, and generalized bone loss with reduced bone mass. In rheumatoid synovium, activated T cells and fibroblasts express RANKL. TNF-α and IL-1β are also overproduced in synovium. TNF-α and IL-1 β, acting in concert with RANKL, can powerfully promote osteoclast recruitment, activation, and osteolysis in RA [55]. In the synovium of patients with RA, NF-κB was present in most macrophages within the lining and sublining lesions throughout the synovium, including endothelial cells [56,57]. CIA is an autoimmune model that in many ways resembles RA. Immunization of genetically susceptible rodents with type II collagen leads to the development of severe polyarticular arthritis mediated by an autoimmune response. Just as in RA, synovitis and erosions of cartilage and bone are hallmarks of CIA [58]. In the present study, direct injection of RNODN in arthritic joints of rats with CIA led to an amelioration of arthritis and decreased the number of TRAP-positive cells in the synovium. The strategy of naked RNODN transfer into the joint implies a potential for future clinical treatment.

Conclusion

RNODN showed higher resistance to exonuclease and higher binding activity on NF-κB than did PNODN. Differentiation and calcium resorption were suppressed by treatment with RNODN, by preventing NFATc1 expression. Joint destruction and osteoclast activity were significantly suppressed by intra-articular injection of RNODN.

These data suggest that RNODNs inhibit the induction and activity of osteoclasts and that the direct injection of RNODNs into the joints might be an effective strategy for the treatment of arthritis.

Competing interests

The authors declare that they have no competing interests.

Authors' contributions

YK performed molecular and animal experiments, measurements and evaluation of the data, and statistical analyses. TT supervised the study design, the interpretation of data, and the writing of the manuscript. TN conceived and participated in the experimental design of the study. RM and HY supervised the study design and gave valuable advice to YK. All authors read and approved the final manuscript.

Additional files

The following Additional files are available online:

Additional File 1

A PDF containing a supplementary figure that demonstrates that there is no activity in the nuclear extracts leading to time-dependent degradation of DNA. See http://www.biomedcentral.com/content/supplementary/ar1980-S1.pdf

Additional File 2

A PDF containing a supplementary figure that examines the effects of RSODN and RNODN on cell growth. See http://www.biomedcentral.com/content/supplementary/ar1980-S2.pdf

Acknowledgements

We wish to thank Tsuyoshi Tajima, Hideaki Sato, and Masafumi Yoshino for their excellent technical assistance. This study was supported in part by grants from the Ministry of Education, Culture, Sports, Science, and Technology of Japan, and the Ministry of Health, Labour and Welfare of Japan.

References

1. Teitelbaum SL: **Bone resorption by osteoclasts.** *Science* 2000, **289**:1504-1508.
2. Yasuda H, Shima N, Nakagawa N, Yamaguchi K, Kinosaki M, Goto M, Mochizuki SI, Tsuda E, Morinaga T, Udagawa N, *et al.*: **A novel molecular mechanism modulating osteoclast differentiation and function.** *Bone* 1999, **25**:109-113.
3. Suda T, Takahashi N, Udagawa N, Jimi E, Gillespie MT, Martin TJ: **Modulation of osteoclast differentiation and function by the new members of the tumor necrosis factor receptor and ligand families.** *Endocr Rev* 1999, **20**:345-357.
4. Yao GQ, Sun BH, Hammond EE, Spencer EN, Horowitz MC, Insogna KL, Weir EC: **The cell-surface form of colony-stimulating factor-1 is regulated by osteotropic agents and supports formation of multinucleated osteoclast-like cells.** *J Biol Chem* 1998, **273**:4119-4128.
5. Shigeyama Y, Pap T, Kunzler P, Simmen BR, Gay RE, Gay S: **Expression of osteoclast differentiation factor in rheumatoid arthritis.** *Arthritis Rheum* 2000, **43**:2523-2530.
6. Kong YY, Yoshida H, Sarosi I, Tan HL, Timms E, Capparellic , Morony S, Oliveira-dos-Santos AJ, Van G, Itie A, *et al.*: **OPGL is a key regulator of osteoclastogenesis, lymphocyte development and lymph-node organogenesis.** *Nature* 1999, **397**:315-323.
7. Hsu H, Lacey DL, Dunstan CR, Solovyev I, Colombero A, Timms E, Tan HL, Elliott G, Kelley MJ, Sarosi I, *et al.*: **Tumor necrosis factor receptor family member RANK mediates osteoclast differentiation and activation induced by osteoprotegerin ligand.** *Proc Natl Acad Sci USA* 1999, **96**:3540-3545.
8. Lacey DL, Timms E, Tan HL, Kelley MJ, Dunstan CR, Burgess T, Elliott R, Colombero A, Elliott G, Scully S, *et al.*: **Osteoprotegerin ligand is a cytokine that regulates osteoclast differentiation and activation.** *Cell* 1998, **93**:165-176.
9. Wei S, Teitelbeum SL, Wang MW-H, Ross FP: **Receptor activator of nuclear factor-κB ligand activates nuclear factor-κB in osteoclast precursors.** *Endocrinology* 2001, **142**:1290-1295.
10. Boyce BF, Xing L, Franzoso G, Siebenlist U: **Required and nonessential functions of nuclear factor-kappa B in bone cells.** *Bone* 1999, **25**:137-139.
11. Jimi E, Aoki K, Saito H, Acquisto FD, May MJ, Nakamura I, Sudo T, Kojima T, Okamoto F, Fukushima H, *et al.*: **Selective inhibition of NF-κB blocks osteoclastogenesis and prevents inflammatory bone destruction *in vivo*.** *Nat Med* 2004, **10**:617-624.
12. Bharti AC, Takada Y, Aggarwal BB: **Curcumin (diferuloylmethane) inhibits receptor activator of NF-κB ligand-induced NF-κB activation in osteoclast precursors and suppresses osteoclastogenesis.** *J Immunol* 2004, **172**:5940-5947.
13. Franzoso G, Carlson L, Xing L, Poljak L, Shores EW, Brown KD, Leonardi A, Tran T, Boyce BF, Siebenlist U: **Requirement for NF-κB in osteoclast and B-cell development.** *Genes Dev* 1997, **11**:3482-3496.
14. Iotsova V, Caamano J, Loy J, Yang Y, Lewin A, Bravo R: **Osteopetrosis in mice lacking NF-κB1 and NF-κB2.** *Nat Med* 1997, **3**:1285-1289.
15. Ruocco MG, Maeda S, Park JM, Lawrence T, Hsu LC, Cao Y, Schett G, Wagner EF, Karin M: **IκB kinase (IKK)β but not IKKα, is a critical mediator of osteoclast survival and is required for inflammation-induced bone loss.** *J Exp Med* 2005, **201**:1677-1687.
16. Takayanagi H, Oda H, Yamamoto S, Kawaguchi H, Tanaka S, Nishikawa T, Koshihara Y: **A new mechanism of bone destruction in rheumatoid arthritis: Synovial fibroblasts induce osteoclastogenesis.** *Biochem Biophys Res Commun* 1997, **240**:279-286.
17. Takano H, Tomita T, Totosaki-Maeda T, Maeda-Taniyama M, Tsuboi H, Takeuchi E, Kaneko M, Shi K, Takahi K, Myoui H, *et al.*: **Comparison of the activities of multinucleated bone-resorbing giant cells derived from CD14-positive cells in the synovial fluids of rheumatoid arthritis and osteoarthritis patients.** *Rheumatology* 2004, **43**:435-441.
18. Gravallese EM, Harada Y, Wang JT, Gorn AH, Thornhill TS, Goldring SR: **Identification of cell types responsible for bone resorption in rheumatoid arthritis and juvenile rheumatoid arthritis.** *Am J Pathol* 1998, **152**:943-951.
19. Lubberts E, Oppers-Walgreen B, Pettit AR, Bersselaar L, Joosten L, Goldring SR, Gravallese EM, Berg WB: **Increase in expression of receptor activator of nuclear factor κB, at sites of bone erosion correlates with progression of inflammation in evolving collagen-induced arthritis.** *Arthritis Rheum* 2002, **46**:3055-3064.
20. Pettit AR, Ji H, von Stechow D, Muller R, Goldring SR, Choi Y, Benoist C, Gravallese EM: **TRANCE/RANKL knockout mice are protected from bone erosion in a serum transfer model of arthritis.** *Am J Pathol* 2001, **159**:1689-1699.
21. Mann MJ, Dzau VJ: **Therapeutic application of transcriptional factor decoy oligonucleotides.** *J Clin Invest* 2000, **106**:1071-1075.
22. Dzau VJ: **Transcription factor decoy.** *Circ Res* 2002, **90**:1234-1236.
23. Morishita R, Sugimoto T, Aoki M, Kida I, Tomita N, Moriguchi A, Maeda K, Sawa Y, Kaneda Y, Higaki J, *et al.*: ***In vivo* transfection of cis element 'decoy'against nuclear factor-κB binding site prevents myocardial infarction.** *Nat Med* 1997, **3**:894-899.
24. Tomita T, Takeuchi E, Tomita N, Morishita R, Kaneko M, Yamamoto K, Nakase T, Seki H, Kato K, Kaneda Y, *et al.*: **Suppressed severity of collagen-induced arthritis by *in vivo* transfection of nuclear factor-κB decoy oligodeoxynucleotides as a gene therapy.** *Arthritis Rheum* 1999, **42**:2532-2542.
25. Tomita T, Takano H, Tomita N, Morishita R, Kaneko M, Shi K, Takahi T, Nakase Y, Kaneda Y, Yoshikawa H, Ochi T: **Transcription factor decoy for NFκB inhibits cytokine and adhesion molecule expressions in synovial cells derived from rheumatoid arthritis.** *Rheumatology* 2000, **39**:749-757.
26. Tomita N, Morishita R, Tomita S, Yamamoto K, Aoki M, Matsushita H, Hayashi S, Higaki J, Ogihara T: **Transcription factor decoy for nuclear factor-κB inhibits tumor necrosis factor-α-induced expression of interleukin-6 and intracellular adhesion molecule-1 in endothelial cells.** *J Hypertens* 1998, **16**:993-1000.
27. Lee IK, Ahn JD, Kim HS, Park JY, Lee KU: **Advantages of the circular dumbbell decoy in gene therapy and studies of gene regulation.** *Curr Drug Targets* 2003, **4**:619-623.
28. Tomita N, Tomita T, Yuyama K, Tougan T, Tajima T, Ogihara T, Morishita R: **Development of novel decoy oligonucleotides: advantages of circular dumb-bell decoy.** *Curr Opin Mol Ther* 2003, **5**:107-112.
29. Hosoya T, Takeuchi H, Kanesaka Y, Yamakawa H, Miyano-Kurosaki N, Takai K, Yamamoto N, Takaku H: **Sequence-specific inhibition of a transcription factor by circular dumbbell DNA oligonucleotides.** *FEBS Lett* 1999, **461**:136-140.
30. Moon IJ, Choi K, Choi YK, Kim JE, Lee Y, Schreiber AD, Park JG: **Potent growth inhibition of leukemic cells by novel ribbon-type antisense oligonucleotides to c-myb1.** *J Biol Chem* 2000, **275**:4647-4653.
31. Trentham D, Townes A, Kang A: **Autoimmunity to type 2 collagen: an experimental model of arthritis.** *J Exp Med* 1977, **146**:857-868.
32. Shiozawa S, Shimizu K, Tanaka K, Hino K: **Studies on the contribution of c-fos/AP-1 to arthritic joint destruction.** *J Clin Invest* 1997, **99**:1210-1216.
33. Rumney SIV, Kool ET: **DNA recognition by hybrid oligother-oligodeoxynucleotide macrocycles.** *Angew Chem Int Ed Engl* 1992, **31**:1617-1619.
34. Gamper HB, Reed MW, Cox T, Virosco JS, Adams AD, Gall AA, Scholler JK, Meyer RB Jr: **Facile preparation of nuclease resistant 3' modified oligodeoxynucleotides.** *Nucleic Acids Res* 1993, **21**:145-150.
35. Takayanagi H, Kim S, Koga T, Nishina H, Isshiki M, Yoshida H, Saiura A, Isobe M, Yokochi T, Inoue J, *et al.*: **Induction and activation of the transcription factor NFATc1(NFAT2) integrate RANKL signaling in terminal differentiation of osteoclasts.** *Dev Cell* 2002, **3**:889-901.
36. Verma IM, Stevenson JK, Schwarz EM, Van Antwerp D, Miyamoto S: **Rel/NF-κB/IκB family: intimate tales of association and dissociation.** *Genes Dev* 1995, **9**:2723-2735.
37. Karin M, Delhase M: **The IκB kinase (IKK) and NF-κB: key elements of proinflammatory signaling.** *Immunology* 2000, **12**:85-98.
38. Jimi E, Nakamura I, Ikebe T, Akiyama S, Takahashi N, Suda T: **Activation of NF-κB is involved in the survival of osteoclasts promoted by interleukin-1.** *J Biol Chem* 1998, **273**:8799-8805.
39. Morishita R, Tomita N, Kaneda Y, Ogihara T: **Molecular therapy to inhibit NFκB activation by transcription factor decoy oligonucleotides.** *Curr Opin Pharmacol* 2004, **4**:139-146.

40. Ahn JD, Morishita R, Kaneda Y, Lee SJ, Kwon KY, Choi SY, Lee KU, Park JY, Moon IJ, Park JG, *et al.*: **Inhibitory effects of novel AP-1 decoy oligodeoxynucleotides on vascular smooth muscle cell proliferation *in vitro* and neointimal formation *in vivo*.** *Circ Res* 2002, **90**:1325-1332.
41. Ahn JD, Morishita R, Kaneda Y, Kim HS, Chang Y-C, Lee K-U, Kim YH, Lee IK: **Novel E2F decoy oligodeoxynucleotides inhibit *in vitro* vascular smooth muscle cell proliferation and *in vivo* neointimal hyperplasia.** *Gene Ther* 2002, **9**:1682-1692.
42. Park KK, Ahn JD, Lee IK, Magae J, Heintz NH, Kwak JY, Lee YC, Cho YS, Kim HC, Chae YM, *et al.*: **Inhibitory effects of novel E2F decoy oligodeoxynucleotides on mesangial cell proliferation by coexpression of E2F/DP.** *Biochem Biophys Res Commun* 2003, **308**:689-697.
43. Brown DA, Kang SH, Gryaznov SM, Dedionisio L, Heidenreich O, Sullivan S, Xu X, Nerenberg MI: **Effect of phosphorothionate modification of oligodeoxynucleotides on specific protein binding.** *J Biol Chem* 1994, **269**:26801-26805.
44. Khaled Z, Benimetskaya L, Zeltser R, Khan T, Sharma HW, Narayanan R, Stein CA: **Multiple mechanisms may contribute to the cellular anti-adhesive effects of phosphorothionate oligodeoxynucleotides.** *Nucleic Acids Res* 1996, **24**:737-745.
45. Chu BCF, Orgel LE: **The stability of different forms of double-stranded decoy DNA in serum and nuclear extracts.** *Nucleic Acids Res* 1992, **20**:5857-5858.
46. Chu BCF, Orgel LE: **Binding of hairpin and dumbbell DNA to transcription factors.** *Nucleic Acids Res* 1991, **19**:6958.
47. Penolazzi L, Lambertini E, Borgatti M, Piva R, Cozzani M, Giovannini I, Naccari R, Siciliani G, Gambari R: **Decoy oligodeoxynucleotides targeting NF-κB transcriptional factors: induction of apoptosis in human primary osteoclasts.** *Biochem Pharmacology* 2003, **66**:1189-1198.
48. Miyazaki T, Katagiri H, Kanegae Y, Takayanagi H, Sawada Y, Yamamoto A, Pando MP, Asano T, Verma IM, Oda H, *et al.*: **Reciprocal role of ERK and NF-κB pathways in survival and activation of osteoclasts.** *J Cell Biol* 2000, **148**:333-342.
49. Ishikawa T, Kamiyama M, Tani-ishii N, Suzuki H, Ichikawa Y, Hamaguchi Y, Momiyama N, Shimada H: **Inhibition of osteoclast differentiation and bone resorption by cathepsin K antisense oligonucleotides.** *Mol Carcinog* 2001, **32**:84-91.
50. Yakubov LA, Deeva EA, Zarytova VF, Ivanova EM, Ryte AS, Yurchenko LV, Vlassov VV: **Mechanism of oligonucleotide uptake by cells: involvement of specific receptors?** *Proc Natl Acad Sci USA* 1989, **86**:6454-6458.
51. Loke SL, Stein CA, Zhang XH, Mori K, Nakanishi M, Subasinghe C, Cohen JS, Neckers LM: **Characterization of oligonucleotide transport into living cells.** *Proc Natl Acad Sci USA* 1989, **86**:3474-3478.
52. Wu-Pong S: **Alternative interpretations of the oligonucleotide transport literature: insights from nature.** *Adv Drug Deliv Rev* 2000, **44**:59-70.
53. Zhou B, Cron RQ: **Regulation of the murine Nfatc1 gene by NFATc2.** *J Biol Chem* 2002, **277**:10704-10711.
54. Takatsuna H, Asagiri M, Kubota T, Oka K, Osada T, Sugiyama C, Saito H, Aoki K, Ohya K, Takayanagi H, *et al.*: **Inhibition of RANKL-induced osteoclastogenesis by (-)-DHMEQ, a novel NF-κB inhibitor, through downregulation of NFATc1.** *J Bone Miner Res* 2005, **20**:653-662.
55. Romas E, Gillespie MT, Martin TJ: **Involvement of receptor activator of NF-κB ligand and tumor necrosis factor-α in bone destruction in rheumatoid arthritis.** *Bone* 2002, **30**:340-346.
56. Marok R, Winyard PG, Coumbe A, Kus ML, Gaffney K, Blades S, Mapp PI, Morris CJ, Blake DR, Kaltschmidt C, *et al.*: **Activation of the transcription factor nuclear factor-κB in human inflamed synovial tissue.** *Arthritis Rheum* 1996, **39**:583-591.
57. Handel ML, McMorrow LB, Gravallese EM: **Nuclear factor-κB in rheumatoid synovium.** *Arthritis Rheum* 1995, **38**:1762-1770.
58. Myers LK, Rosloniec EF, Cremer MA, Kang AH: **Collagen-induced arthritis, an animal model of autoimmunity.** *Life Sci* 1997, **61**:1861-1878.

ELSEVIER

The Spine Journal 6 (2006) 325–329

THE SPINE JOURNAL

Paraparesis due to exacerbation of preexisting spinal pseudoarthrosis following infliximab therapy for advanced ankylosing spondylitis

Hironobu Sakaura, MD*, Noboru Hosono, MD, PhD, Yoshihiro Mukai, MD, Ryutaro Fujii, MD, Hideki Yoshikawa, MD, PhD

Department of Orthopedic Surgery, Osaka University, Graduate School of Medicine, 2-2 Yamada-oka, Suita, Osaka 565-0871, Japan

Received 5 April 2005; accepted 31 October 2005

Abstract

BACKGROUND CONTEXT: Recent reports have described the long-term efficacy and safety of infliximab as a treatment for ankylosing spondylitis (AS). The most important adverse effects of infliximab are infections, malignancies, autoimmunities, and hypersensitivity reactions. There has never been a reported case of paraparesis after infliximab therapy for AS.

PURPOSE: To describe a case with paraparesis caused by rapid exacerbation of preexisting spinal pseudoarthrosis after infliximab therapy for advanced AS.

STUDY DESIGN/SETTING: Case report/Osaka University Graduate School of Medicine, Suita, Japan.

PATIENT SAMPLE: A 55-year-old man with a 27-year history of AS.

OUTCOME MEASURES: Case report.

METHODS: A 55-year-old man with a 27-year history of AS was treated with infliximab, which provided considerable pain relief and improvement of activities of daily living. However, as the patient resumed vigorous daily activity, he felt back pain and subsequently developed paraparesis. Radiographs showed rapid exacerbation of preexisting spinal pseudoarthrosis at the T11–T12 level after infliximab therapy.

RESULTS: After laminectomy and posterolateral fusion, the back pain and paraparesis improved sufficiently to allow independent walking, but moderate bladder dysfunction persisted.

CONCLUSIONS: Although this patient could have certainly become myelopathic over time without undergoing infliximab therapy, the patient's history and radiographic course suggest that suppression of inflammation by infliximab improved his activities of daily living, which paradoxically exacerbated preexisting spinal pseudoarthrosis and quickened the onset of subsequent myelopathy.

Keywords: Ankylosing spondylitis/complications; Monoclonal antibodies/therapeutic use; Antirheumatic agents/therapeutic use; Paraparesis/etiology

Introduction

Infliximab (Remicade; Centocor, Inc., Malvern, PA) is a chimeric IgG_1 monoclonal antibody that binds to tumor necrosis factor alpha (TNFα) and inhibits its biological effect. The therapeutic effect of infliximab has been established for rheumatoid arthritis, psoriasis, and Crohn's disease [1]. Recently, infliximab has also been approved for treatment of ankylosing spondylitis (AS) in Europe, after confirmation of the long-term efficacy and safety of infliximab for treatment of AS [1–3]. Infections, autoimmunities, and hypersensitivity reactions are well-known major adverse effects of infliximab [1–3]. However, paraparesis has never been observed as an adverse effect of infliximab therapy for AS. This report describes a rare case of paraparesis following treatment with infliximab for advanced AS.

Case report

A 55-year-old man with a 27-year history of AS was referred to our orthopedic clinic with progressive gait

FDA device/drug status: not applicable.

Nothing of value received from a commercial entity related to this manuscript.

* Corresponding author. Department of Orthopedic Surgery, Osaka University, Graduate School of Medicine, 2-2 Yamada-oka, Suita, Osaka 565-0871, Japan. Tel.: +81-6-6879-3552; fax: +81-6-6879-3559.

E-mail address: sakaurah@ort.med.osaka-u.ac.jp (H. Sakaura)

1529-9430/06/$ – see front matter
doi:10.1016/j.spinee.2005.10.012

disturbance and urinary retention. Three months before referral, he began receiving intravenous infliximab at a dose of 5 mg/kg every 2 weeks (induction phase) to treat refractory AS. Infliximab provided considerable pain relief and suppression of disease activity. However, as the patient resumed vigorous daily activities, he began to feel backache radiating to his left flank and crepitation in his back at movement without any preceding trauma. Over a 3-week period, his gait gradually deteriorated, and he developed urinary retention and paresthesia in the sacral area (Fig. 1).

At clinical examination, the patient reported percussion tenderness in the thoracolumbar transitional area. He could hardly walk without the support of handrails or a cane. Neurological examination revealed hyperreflexia and moderate motor weakness in his lower extremities. The patient had hypesthesia in the lower extremities and anesthesia in the sacral area. Anteroposterior and lateral radiographs showed severe spinal pseudoarthrosis at the T11–T12 level, with vacuum phenomenon in the intervertebral disc space and sclerotic change of the vertebral bodies adjacent to the diseased disc, and all other segments were ankylosed (Fig. 2a, b). Hypermobility between T11 and T12 was observed on the lateral radiographs in flexion and extension position (Fig. 2c, d). Retrospective examination of radiographs revealed that initial signs of spinal pseudoarthrosis were present 2 months before the beginning of infliximab therapy (Fig. 2e, f). Magnetic resonance imaging showed decreased signal intensity in the disc space and the adjacent margins of T11 and T12 on both T1- and T2-weighted images. The spinal cord sustained compression by protrusion of the disc anteriorly and by hypertrophy of yellow ligaments posteriorly (Fig. 3a, b). Computed tomography showed a fracture of the left pars interarticularis at T12 and calcification of the hypertrophied yellow ligaments (Fig. 3c).

At surgery, the nonankylosed right facet joint at T11–T12 and pseudoarthrosis at the left pars interarticularis of the T12 lamina were confirmed; these conditions resulted in considerable instability at the T11–T12 level. Laminectomy of T11 and T12, and posterolateral fusion from T10 to L1 were performed using a pedicle screw system (Fig. 4a, b).

After surgery, the patient reported great pain relief in his back, and exhibited full recovery of motor strength in the lower extremities. At the latest follow-up 4 months after surgery, he could walk independently without pain, although moderate bladder dysfunction persisted.

Discussion

Since the first description of a destructive discovertebral lesion complicating AS, by Andersson in 1937 [4], such destructive lesions, known as spinal pseudoarthrosis, have come to be recognized as one of the most important complications of advanced AS [4–22]. The exact pathogenesis of these lesions remains controversial. There is debate as to whether inflammatory changes or mechanical stresses play the key role in the development of these lesions [5–9,15,17,19,21,22].

In the present case, inflammatory activity of AS was apparently controlled by administration of infliximab, which provided dramatic pain relief and improvement of activities of daily living. Unfortunately, the patient's increased activity most likely led to spinal instability at the remaining

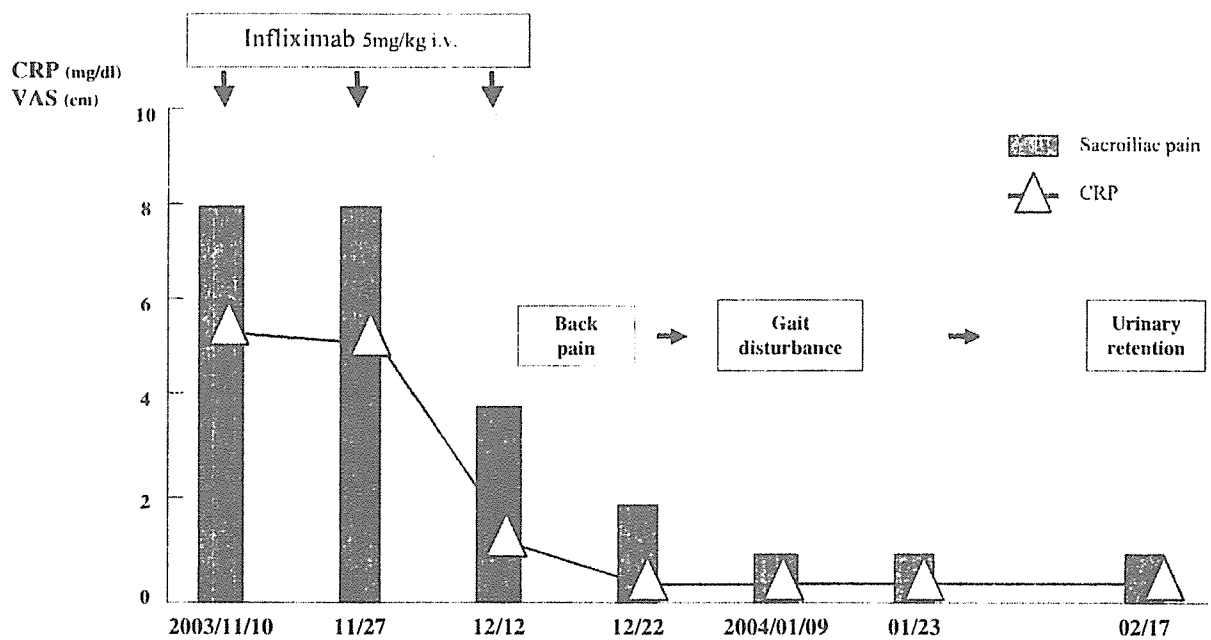

Fig. 1. Clinical course following infliximab therapy is summarized. After the decrease in sacroiliac pain and serum C-reactive protein (CRP), the patient developed back pain and subsequently paraparesis. VAS=visual analogue scale.

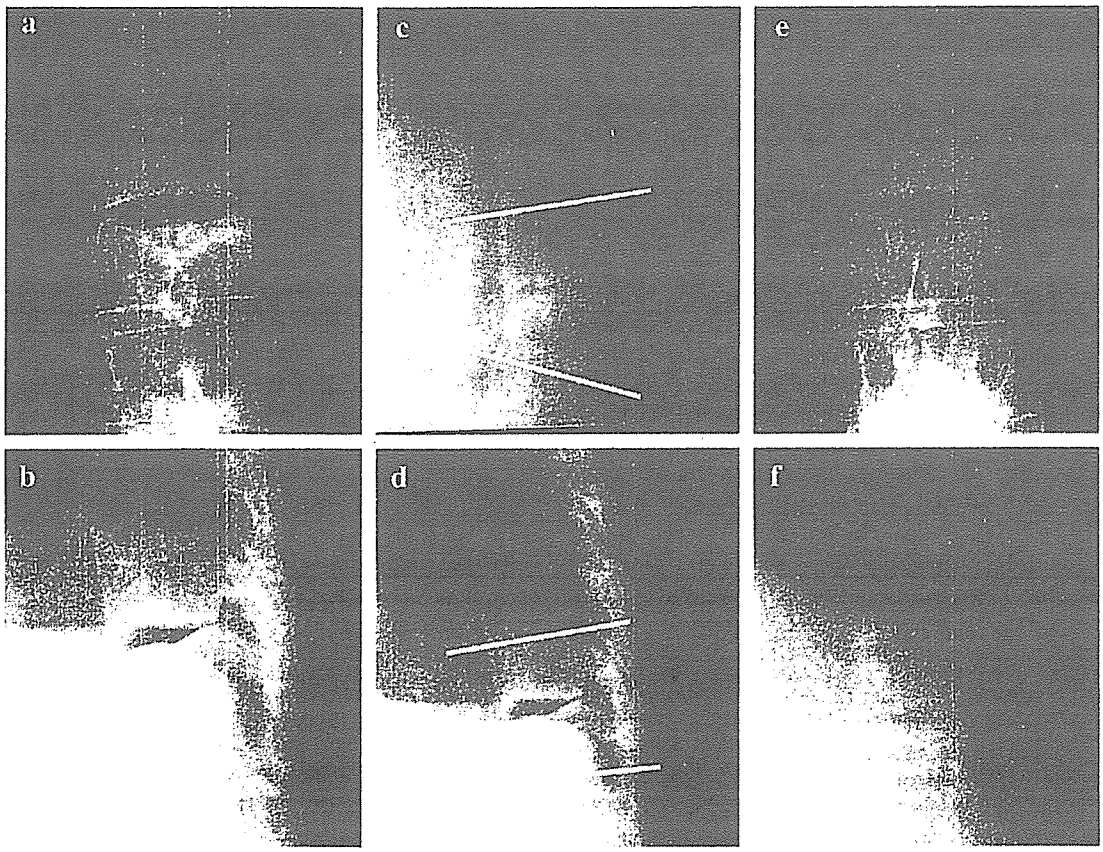

Fig. 2. Radiographs of the thoracolumbar junction. (a, b) At referral (2 months after the third infusion of infliximab). Vacuum phenomenon in the intervertebral space and sclerosis of the adjacent margins of T11 and T12 are visible. (c, d) Lateral radiographs in flexion and extension positions at referral. Hypermobility between T11 and T12 is indicated (range of motion, 12.2°). (e, f) Two months before infliximab therapy. The initial changes of pseudoarthrosis are visible.

mobile segment of the spine, resulting in serious paraparesis. Retrospective examination of radiographs confirmed significant exacerbation of preexisting spinal pseudoarthrosis after the beginning of infliximab therapy. Although this patient could have certainly become myelopathic over time without undergoing infliximab therapy, the patient's history and radiographic course suggest that suppression of inflammation by infliximab improved his activities of daily living, which paradoxically exacerbated the preexisting spinal pseudoarthrosis and contributed to the development of subsequent paraparesis.

Anti-TNFα agents such as infliximab have provided a new approach to the treatment of AS; no disease-modifying antirheumatic drugs are effective against AS [1–3]. Recent reports indicate that infliximab provides long-term efficacy and safety in the treatment of AS [2,3]. Although severe adverse effects of infliximab are rare, some physicians are concerned about the possibility of the following types of adverse events: infections including sepsis and tuberculosis; malignancies such as lymphoma; hematological disorders such as pancytopenia; demyelinating neuropathy; congestive heart failure; elevation of liver enzymes; lupus and vasculitis; autoimmunities and hypersensitivity reactions [1–3]. Braun et al. reported that continuous infliximab treatment for refractory AS for 54 weeks resulted in significant and durable pain relief, improvement in physical function, and decrease in disease activity. Six of their 69 patients discontinued infliximab therapy because of the following adverse events: systemic tuberculosis, leukopenia, possibly antinuclear antibody–associated peripheral arthritis, lupus-like rash, and liver function abnormalities [2]. However, there have been no reported cases of paraparesis due to rapid exacerbation of spinal pseudoarthrosis after infliximab therapy for AS.

Spinal pseudoarthrosis is not an uncommon complication of AS [4–22]; the estimated prevalence of this complication ranges from 1% to 16% [17,22]. Severe neurological deficits are rare clinical manifestations of spinal pseudoarthrosis. Most patients with pseudoarthrosis only exhibit localized backache, which is often misinterpreted as a common symptom of AS. Fang et al. reported that only 4 of their 35 patients with spinal pseudoarthrosis had neurological symptoms, and the remaining 31 patients complained only of back pain [17]. For these reasons, this complication can be easily overlooked by physicians, possibly resulting in more serious consequences. Now that infliximab has

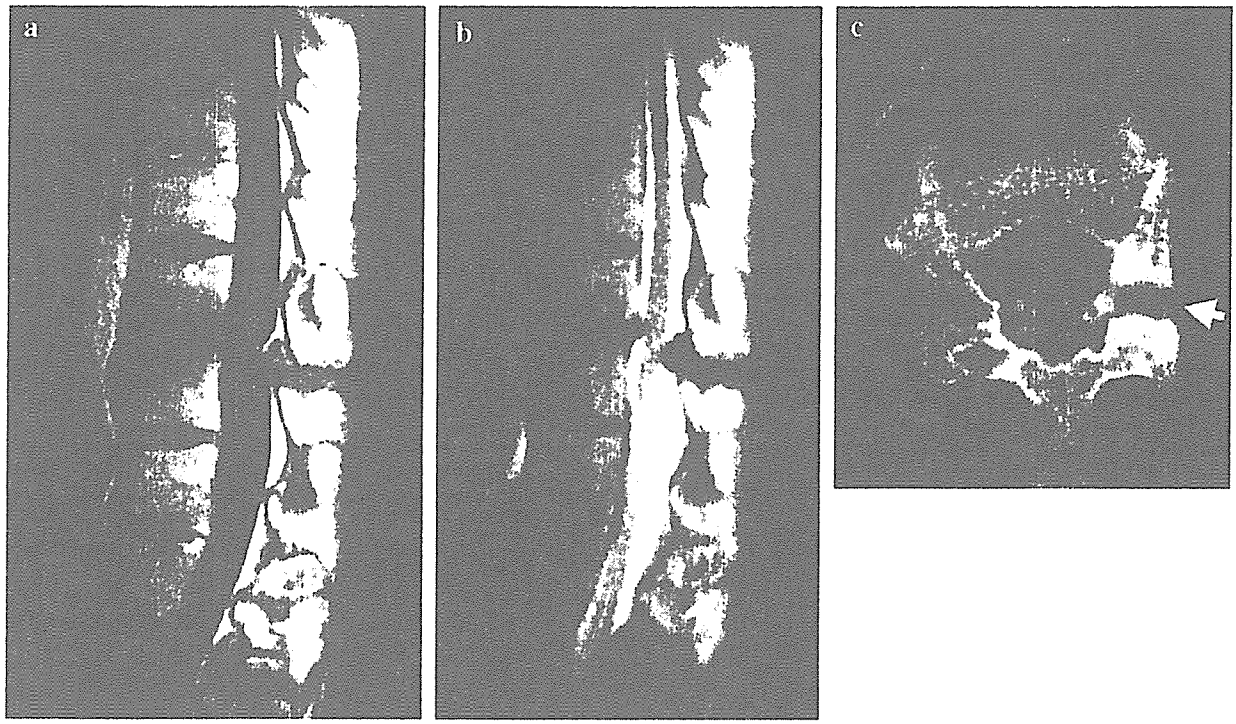

Fig. 3. Before surgery, magnetic resonance imaging showed decreased signal intensity at the disc space and the adjacent margins between T11 and T12 on both the (a) T1- and (b) T2-weighted images. The dural sac was compressed by the protruding disc and the hypertrophied yellow ligaments. (c) Computed tomogram showed a fracture of the left pars interarticularis at T12 (arrow) and calcification of the hypertrophied yellow ligaments.

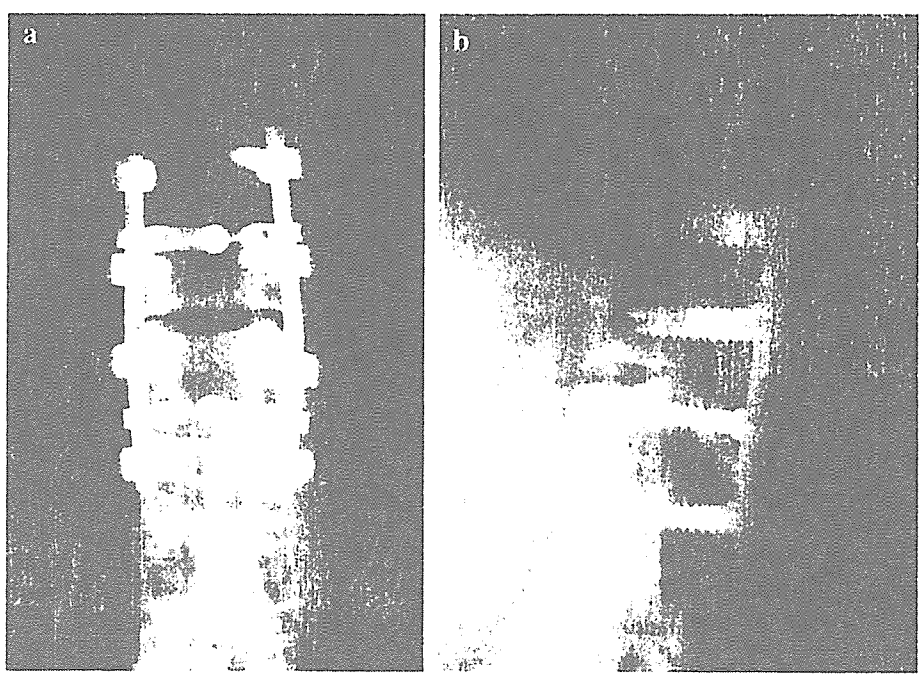

Fig. 4. Postoperative radiographs of the thoracolumbar spine. After laminectomy of T11 and T12, posterolateral fusion from T10 to L1 was performed using a pedicle screw system. (a) Anteroposterior view. (b) Lateral view.